SIMULATION OF THE FRACTIONAL DERIVATIVE OPERATOR $\sqrt{s}$ AND THE FRACTIONAL INTEGRAL OPERATOR $1/\sqrt{s}$

by

GORDON EUGENE CARLSON

B. S., Kansas State University
of Agriculture and Applied Science, 1959

A MASTER'S REPORT

submitted in partial fulfillment of the

requirements for the degree

MASTER OF SCIENCE

Department of Electrical Engineering

KANSAS STATE UNIVERSITY
OF AGRICULTURE AND APPLIED SCIENCE

1960

TABLE OF CONTENTS

INTRODUCTION

The purpose of this paper is to approximate the operator $\sqrt{s}$ and $1/\sqrt{s}$. A necessary preliminary to the approximating procedures is a study of the linear adaptive servo. The linear adaptive servo is analyzed with both derivative feedback control and integral feedback control.

If the transfer function for this servo has large feedback gain, then the Newton and Lanczos approximations to the fractional derivative and fractional integral operators may be simulated. It is then natural to consider their operational amplifier counterparts. The operational amplifiers for performing these simulations are exhibited. A close tie is also developed with the operational amplifier simulations using the theory of characteristic impedances to arrive at the approximations to the fractional derivative and the fractional integral.

Several applications of these fractional operators are discussed. Analog computer simulations of these approximate functions are made, and the use of these fractional operators as servo compensation means is shown.

THE LINEAR ADAPTIVE SERVO

Work on an adaptive control system has been under way at Cornell Aeronautical Laboratories since 1955. The work was started by Campbell (1) and has been continued to the present. The system developed by Cornell Aeronautical Laboratories differs greatly from most of the adaptive control systems since it is a linear system. The system does not change any of its parameters to compensate from changes in the system, but instead modifies the input to the control element by subtracting from the actual input the deviation of the control element from the model.

The block diagram of the system used by Cornall Aeronautical Laboratories is shown in Fig. 1.[1] The particular element which they sought to control was an aircraft, but the controlled element A in Fig. 1 could be any system to which feedback control is applicable. In order to better understand this control system shown, it is first necessary to apply some topological reduction to the block diagram. Through this method the overall transfer function of the system may be evaluated. Figure 2 shows another block diagram of the reduced system. This shows that the system could be regarded as a simple feedback system with a prefiltering of the input signal. The overall transfer function of the system is

$$\frac{\text{output}}{\text{input}} = (1 + MB) \cdot \frac{A}{1 + AB} \qquad (1)$$

As can be seen readily from the transfer function, the output of the system will approach the output of the model if the gains B and AB are made very large.

The model itself is nothing more than a holding filter which has been approximated by a second order transfer function. The model used by Cornell Aeronautical Laboratories had a natural

[1]All figures for this report are in the Appendix.

frequency of 0.5 cps and a damping factor which was 0.7 of the critical damping factor. These values were found to be the most desirable from preferences indicated by test pilots who had flown variable stability aircraft.

The feedback element used by Cornell Aeronautical Laboratories had a transfer function of $B_o\ (1 + \tau s)$. This gives two variables in the feedback loop which can be adjusted to improve performance. The value of the time constant in this feedback transfer function was $\tau = 0.2$.

Using the model and the feedback element as used by Cornell, and also using the assumption that the element to be controlled can be represented by a second order transfer function in the short period frequency range, the system can be analyzed somewhat more precisely. In equation form, the above assumptions are

$$A(s) = \frac{A_o}{1 + \frac{2\zeta_A}{\omega_A} s + \frac{1}{\omega_A^2} s^2} \qquad (2)$$

$$B(s) = B_o(1 + \tau s) \qquad (3)$$

$$M(s) = \frac{M_o}{1 + \frac{2\zeta_M}{\omega_M} s + \frac{1}{\omega_M^2} s^2} \qquad (4)$$

The transfer function again was

$$\frac{\text{output}}{\text{input}} = \frac{1 + MB}{1 + AB} \cdot A \qquad (5)$$

Substituting the above values for A, F, and M gives the following equation,

$$T(s) = \frac{1 + \dfrac{M_oB_o(1 + \tau s)}{1 + \dfrac{2\zeta_M}{\omega_M} s + \dfrac{1}{\omega_M^2} s^2}}{1 + \dfrac{A_oB_o(1 + \tau s)}{1 + \dfrac{2\zeta_A}{\omega_A} s + \dfrac{1}{\omega_A^2} s^2}} \cdot \frac{A_o}{1 + \dfrac{2\zeta_A}{\omega_A} s + \dfrac{1}{\omega_A^2} s^2} \qquad (6)$$

which in turn consolidates to

$$T(s) = \frac{1}{1 + \dfrac{2\zeta_M}{\omega_M} s + \dfrac{1}{\omega_M^2} s^2} \cdot \frac{A_o(1 + M_oB_o)}{1 + A_oB_o}$$

$$\cdot \frac{1 + \left(\dfrac{\dfrac{2\zeta_M}{\omega_M} + M_oB_o\tau}{1 + M_oB_o}\right) s + \dfrac{1}{(1 + M_oB_o)\omega_M^2} s^2}{1 + \left(\dfrac{\dfrac{2\zeta_A}{\omega_A} + A_oB_o\tau}{1 + A_oB_o}\right) s + \dfrac{1}{(1 + A_oB_o)\omega_A^2} s^2} \qquad (7)$$

Ideally all coefficients except those of M(s) of the above equation should be one. This is called the ideal condition and it can be achieved. In order to make the third term of the product in equation (7) equal to one, the coefficients of the powers of s must be equal in the numerator and the denominator. Since the constant terms are equal, attention should be turned next to the coefficients of the first power of s. Setting these two coefficients equal gives

$$\frac{\dfrac{2\zeta_M}{\omega_M} + M_oB_o}{1 + M_oB_o} = \frac{\dfrac{2\zeta_A}{\omega_A} + A_oB_o}{1 + A_oB_o} \qquad (8)$$

Solving for B_o gives

$$B_o = \frac{\dfrac{\zeta_A}{\omega_A} - \dfrac{\zeta_M}{\omega_M}}{A_o \dfrac{\zeta_M}{\omega_M} - M_o \dfrac{\zeta_A}{\omega_A} - \dfrac{\tau}{2}(A_o - M_o)} \tag{9}$$

The gain of the feedback element therefore can be related to the gain of the controlled element, the gain of the model, and the damping constants of the controlled element and model. If this value of feedback gain is substituted into the equation (7) representing the transfer function of the system, it becomes

$$T(s) = M \cdot \frac{A_o}{M_o} \frac{\dfrac{\zeta_M}{\omega_M} - \dfrac{\tau}{2}}{\dfrac{\zeta_A}{\omega_A} - \dfrac{\tau}{2}} \cdot \frac{1 + a_1 s + \dfrac{a_2}{\omega_M^2} s^2}{1 + b_1 s + \dfrac{b_2}{\omega_A^2} s^2} \tag{10}$$

Already, $a_1 = b_1$ has been imposed.

Proceeding further, one has

$$a_2 = \frac{1}{1 + M_oF_o} = \frac{A_o \dfrac{\zeta_M}{\omega_M} - M_o \dfrac{\zeta_A}{\omega_A} - \dfrac{\tau}{2}(A_o - M_o)}{\left(\dfrac{\zeta_M}{\omega_M} - \dfrac{\tau}{2}\right)(A_o - M_o)} = \frac{K}{\left(\dfrac{\zeta_M}{\omega_M} - \dfrac{\tau}{2}\right)} \tag{11}$$

$$b_2 = \frac{1}{1 + A_oF_o} = \frac{A_o \dfrac{\zeta_M}{\omega_M} - M_o \dfrac{\zeta_A}{\omega_A} - \dfrac{\tau}{2}(A_o - M_o)}{\left(\dfrac{\zeta_A}{\omega_A} - \dfrac{\tau}{2}\right)(A_o - M_o)}$$

$$= \frac{K}{\left(\dfrac{\zeta_A}{\omega_A} - \dfrac{\tau}{2}\right)} \tag{12}$$

One can conclude from (11) and (12) that

$$a_2 = b_2 \frac{\dfrac{\zeta_A}{\omega_A} - \dfrac{\tau}{2}}{\dfrac{\zeta_M}{\omega_M} - \dfrac{\tau}{2}} \tag{13}$$

To make the last term of the product completely equal requires still one more step, equating the coefficients of the s^2 terms.

Again, the identities

$$\frac{a_2}{\omega_M^2} = \frac{b_2}{\omega_A^2} \tag{14}$$

$$\frac{\omega_A^2 K}{(\dfrac{\zeta_M}{\omega_M} - \dfrac{\tau}{2})} = \frac{\omega_M^2 K}{\dfrac{\zeta_A}{\omega_A} - \dfrac{\tau}{2}} \tag{15}$$

(where the quantity K is found in (11) and (12)) can be manipulated to yield

$$\tau = 2 \cdot \frac{\omega_A \zeta_A - \omega_M \zeta_M}{\omega_A^2 - \omega_M^2} \tag{16}$$

This then specifies the relation between the natural frequencies and damping constants of the model and controlled element, and the time constant τ of the feedback element at the ideal condition. If, then, these conditions are adhered to, the overall transfer function of the system will be

$$T(s) = A_o (\frac{\omega_A}{\omega_M})^2 \cdot (\frac{1}{1 + \dfrac{2\zeta_M}{\omega_M} s + \dfrac{1}{\omega_M^2} s^2}) \tag{17}$$

This transfer function at the ideal condition is the transfer function of the model with a gain factor. The gain factor is dependent upon two of the controlled systems parameters, namely, A_o and ω_A. Therefore any changes in these parameters would cause a change in the overall gain even though B_c and τ were adjusted to the proper values for the ideal condition.

A summary of results is now possible. Whereas the controlled element by itself has three possible parameters, (A_o, ζ_A, ω_A), which can vary, the linear adaptive servo at the ideal condition has three parameters ($A_o\left(\frac{\omega_A}{\omega_M}\right)^2$, ζ_M, ω_M) in which only one, namely, $A_o(\omega_A/\omega_M)^2$, can vary. Therefore a 67 per cent reduction in number of varying parameters has been achieved. It is presupposed that ζ_M and ω_M will not be subjected to any variation and this is achievable. The performance of the model is substituted for the performance of the controlled element except that the overall gain is a function of A_o and ω_A which can vary.

This derivation depends on the ability to change B_o and τ as required if the variables A_o, ω_A, ζ_A should vary. In the particular system proposed by Cornell Aeronautical Laboratories there is no provision to change these parameters. In order to check on the effectiveness of the system to adapt to changes in the controlled element, it becomes necessary to determine what effect these changes will have on the system if deviations from the ideal condition occur. The effect of these changes can be determined by finding the transfer function difference from the ideal condition when A_o, ω_A, and ζ_A deviate from the values used in calculating B_o and τ at the ideal condition. The transfer function from the system with B_o and τ chosen according to their

$$T(s) = A_o\left(\frac{\omega_A}{\omega_M}\right)^2 \left(\frac{1}{1 + \frac{2\zeta_M}{\omega_M}s + \frac{1}{\omega_M^2}s^2}\right) = \left[M(s)\right]\left[\frac{A_o}{M_o}\left(\frac{\omega_A}{\omega_M}\right)^2\right] \quad (18)$$

The transfer function for the system, with changes in A_o, ω_A, and ζ_A, will now be

$$T'(s) = (M)\left[\frac{(A_o + \Delta A_o)(1 + M_oB_o)}{M_o\left[1 + (A_o + \Delta A_o)B_o\right]}\right]$$

$$\left[\frac{1 + \dfrac{\dfrac{2\zeta_M}{\omega_M} + M_oB_o}{1 + M_oB_o}s + \dfrac{1}{(1 + M_oB_o)\omega_M^2}s^2}{1 + \dfrac{\dfrac{2(\zeta_A + \Delta\zeta_A)}{\omega_A + \Delta\omega_A} + (A_o + \Delta A_o)B_o\tau}{1 + (A_o + \Delta A_o)B_o}s + \dfrac{s^2}{(1 + \left[A_o + \Delta A_o\right]B_o)(\omega_A + \Delta\omega_A)^2}}\right] \quad (19)$$

where

$$\tau = 2\left[\frac{\omega_A\zeta_A - \omega_M\zeta_M}{\omega_A^2 - \omega_M^2}\right] \quad (20)$$

and

$$B_o = \frac{\dfrac{\zeta_A}{\omega_A} - \dfrac{\zeta_M}{\omega_M}}{A_o\dfrac{\zeta_M}{\omega_M} - M_o\dfrac{\zeta_A}{\omega_A} - \dfrac{\tau}{2}(A_o - M_o)} = \frac{\omega_M^2 - \omega_A^2}{A_o\omega_A^2 - M\,\omega_M^2} \quad (21)$$

First an analysis will be made to determine what the difference in the steady-state transfer function will be. The difference between the two transfer functions in the steady-state condition is,

$$T'(o) - T(o) = M_o\left[\frac{(A_o + \Delta A_o)(1 + M_oB_o)}{1 + (A_o + \Delta A_o)B_o} - A_o\left(\frac{\omega_A}{\omega_M}\right)^2\right] \quad (22)$$

which reduces to

$$T'(o) - T(o) = M_o \Delta A_o \left(\frac{\omega_A^2}{\omega_M^2}\right)$$

$$\left[\frac{1 - \dfrac{A_o}{A_o - M_o}\left(\dfrac{\omega_M^2 - \omega_A^2}{\omega_M^2}\right)}{1 - \dfrac{\Delta A_o}{A_o - M_o}\left(\dfrac{\omega_M^2 - \omega_A^2}{\omega_M^2}\right)}\right] \tag{23}$$

This shows that the steady-state difference of the transfer functions is directly proportional to the change in the controlled system gain, ΔA_o, and to the ratio of the natural frequencies squared. In a first order approximation, the steady-state difference is $M_o \Delta A_o \left(\frac{\omega_A}{\omega_M}\right)^2$. Since ω_A will typically be larger than ω_M, the difference in the transfer functions at steady state will be larger than the change in gain ΔA_o. Therefore, at steady-state conditions, the linear adaptive servo will not be immune to changes in the gain, A_o, and the angular frequency, ω_A, of the controlled element.

One other fact should be noted before leaving the steady-state conditions. This is the effect that the choice of M_o has on the steady-state difference in the transfer functions. Choose M_o in the following manner.

$$M_o = A_o \left(\frac{\omega_A}{\omega_M}\right)^2 \tag{24}$$

Then by substitution into the equation for the steady-state difference of the transfer functions (23), the following interesting result is noted.

$$T'(o) - T(o) = M_o \Delta A_o \left(\frac{\omega_A^2}{\omega_M^2}\right) \left[\frac{1 - \dfrac{A_o}{A_o}}{1 + \dfrac{\Delta A_o}{A}} \right] = 0 \qquad (25)$$

Therefore with this proper choice of M_o, there is no steady-state difference regardless of what changes there might be in the parameters A_o, ω_A, and ζ_A. This choice of M_o also entails a change in B_o since B_o depends on M_o and the equation of the difference of the transfer functions was derived using B_o.

$$B_o = \frac{\omega_M^2 - \omega_A^2}{A_o\omega_A^2 - M_o\omega_M^2} = \frac{\omega_M^2 - \omega_A^2}{A_o\omega_A^2 - A_o\omega_A^2} = \infty \qquad (26)$$

Therefore for the above complete independence of the steady-state condition with respect to the changing system parameters, the gain of the feedback loop would have to be infinite. This could not be realized, of course, but at least the model gain, M_o, could be adjusted to give some maximum practical value of feedback gain and still keep the proper relationship between the feedback gain and the other parameters so as to give an output with the model's characteristics.

The system will now be analyzed to determine the difference in the transfer functions at time equal to zero. In other words, the time at which a command is put into the system. The difference between the two transfer functions at time equal to zero may be expressed as follows.

$$T'(\infty) - T(\infty) = \lim_{s\to\infty} \frac{M_o\omega_M^2}{s^2} \left\{ \left[\frac{(A_o + \Delta A_o)(1 + M_oB_o)}{1 + (A_o + \Delta A_o)B_o} \right] \right.$$

$$\left. \left[\frac{1 + (A_o + \Delta A_o)B_o}{1 + M_oB_o} \right] \left[\frac{\omega_A + \Delta \omega_A}{\omega_M} \right]^2 - A_o \left(\frac{\omega_A}{\omega_M}\right)^2 \right\} \tag{27}$$

which may be consolidated to

$$T'(\infty) - T(\infty) = \lim_{s\to\infty} \frac{M_o}{s^2} A_o \left[2\, \omega_A \Delta\omega_A + (\Delta\,\omega_A)^2 \right]$$

$$+ \Delta A_o(\omega_A + \Delta\,\omega_A)^2 \tag{28}$$

Assuming that the square of $\Delta\,\omega_A$ is negligible, the following is obtained:

$$T'(\infty) - T(\infty) = \lim_{s\to\infty} \frac{M_oA_o}{s^2} (2\, \omega_A\, \Delta\, \omega_A)$$

$$+ \Delta A_o(\omega_A^2 + 2\omega_A \Delta \omega_A) \tag{29}$$

Now if ΔA_o is taken to be some increment of A_o, and $\Delta\omega_A$ is some increment of ω_A. this then defines α and β by

$$\Delta A_o = \alpha A_o, \qquad \Delta \omega_A = \beta\, \omega_A \tag{30}$$

and equation (29) can be written as

$$T'(\infty) - T(\infty) = \lim_{s\to\infty} \frac{M_o}{s^2} \cdot A_o\omega_A^2 \left[\alpha + 2\,\beta(1 + \alpha)\right] \tag{31}$$

One can now conclude that none of the parameters of equation (31) can be chosen to aid the limit process is zeroing the response at initial time. It should be observed that relative changes in ω_A produces a greater variation in $\left[\alpha + 2\,\beta(1 + \alpha)\right]$ than relative changes in A.

THE LINEAR ADAPTIVE SERVO WITH INTEGRAL CONTROL

Campbell (1) mentions that the adaptive servo might also have some possibilities with integral control in the feedback loop, but he does not choose to investigate this case. This is done now.

Redefine the feedback so it contains integral control instead of derivative control. The transfer function of the system is still

$$T = \frac{1 + MB}{1 + AB} \cdot A \tag{32}$$

wherein

$$A(s) = \frac{A_o}{1 + \frac{2\zeta_A}{\omega_A} s + \frac{1}{\omega_A^2} s^2} \tag{33}$$

$$B(s) = B_o\left(1 + \frac{\omega_B}{s}\right) \tag{34}$$

$$M(s) = \frac{M_o}{1 + \frac{2\zeta_M}{\omega_M} s + \frac{1}{\omega_M^2} s^2} \tag{35}$$

Substituting the values of A, B, and M into the equation for the transfer function gives the equation

$$T(s) = M(s) \cdot \frac{1 + \frac{1+M_oB_o}{M_oB_o\omega_B} s + \frac{2\zeta_M}{\omega_M M_o B_o \omega_B} s^2 + \frac{1}{\omega_M^2 M_o B_o \omega_B} s^3}{1 + \frac{1+A_oB_o}{A_oB_o\omega_B} s + \frac{2\zeta_A}{\omega_A A_o B_o \omega_B} s^2 + \frac{1}{\omega_A^2 A_o B_o \omega_B} s^3} \tag{36}$$

Several things can now be noted. First, the steady-state transfer function is the constant gain M_o. Since the parameters of the model can be made to remain constant, the steady-state transfer function will remain the same regardless of changes in the controlled system's parameters. Secondly, the transfer function at the initial time, or the time that a signal is put into the system, is as follows.

$$T(\infty) = \lim_{s \to \infty} A_o \omega_A{}^2/s^2 \tag{37}$$

This transfer function differs from the transfer function of the model at initial time by a gain factor of $\dfrac{A_o \omega_A{}^2}{M_o \omega_M{}^2}$. As can be readily seen, this gain is affected by changes in the parameters A_o and ω_A. Lastly, the overall transfer function of the system cannot be made equal to the transfer function of the model by any choice of feedback parameters. The overall system can approach the characteristics of the model only by choosing B_o and ω_B very high. These can be chosen large enough in practice to make the performance close to the performance of the model.

It is necessary to check the changes in performance of this system as parameters in the controlled element vary. The transfer function after changes in the controlled element parameters would be as follows.

$$T'(s) = M(s) \frac{1 + n_1 s + n_2 s^2 + n_3 s^3}{1 + d_1 s + d_2 s^2 + d_3 s^3} \tag{38}$$

wherein

$$n_1 = \frac{1 + M_o B_o}{M_o B_o \omega_B} \tag{39}$$

$$n_2 = \frac{2\zeta_M}{\omega_M M_o B_o \omega_B} \qquad (40)$$

$$n_3 = \frac{1}{\omega_M^2 M_o B_o \omega_B} \qquad (41)$$

$$d_1 = \frac{1 + (A_o + \Delta A_o)B_o}{(A_o + \Delta A_o)B_o\omega_B} \qquad (42)$$

$$d_2 = \frac{2(\zeta_A + \Delta\zeta_A)}{(\omega_A + \Delta\omega_A)(A_o + \Delta A_o)B_o\omega_B} \qquad (43)$$

$$d_3 = \frac{1}{(\omega_A + \Delta\omega_A)^2\ (A_o + \Delta A_o)B_o\omega_B} \qquad (44)$$

The difference in the transfer functions before and after changes in controlled element parameters can now be evaluated. The difference in the steady-state transfer functions is expressed below.

$$T'(o) - T(o) = M_o - M_o = 0 \qquad (45)$$

Therefore any change in the controlled element's parameters will not affect the steady-state error transfer function from being zero.

It has been shown before that the transfer function at the initial point of an input signal, or time equal to zero, is equal to $\lim\limits_{s \to \infty} A_o\omega_A{}^2/s^2$. The difference in this transfer function before and after changes in the controlled element parameters may be expressed as follows.

$$T'(\infty) - T(\infty) = \lim_{s \to \infty} \frac{1}{s^2}\left[(A_o + \Delta A_o)(\omega_A + \Delta\omega_A)^2 - A_o\omega_A{}^2\right] \qquad (46)$$

This difference in transfer functions can be seen to be nearly the same as the difference in transfer functions for the derivative feedback case under initial conditions. The only difference in the two cases is the gain factor M_o. Therefore if the gain of the model M_o were larger than one, the integral feedback system would show some improvement over the derivative feedback system under initial conditions. If the model gain, M_o, were equal to one, the two types of systems would show the same error under initial conditions.

NEWTON AND LANCZOS APPROXIMATIONS OF $\sqrt{s}$ and $1/\sqrt{s}$

The transfer function of the linear adaptive servo leads to an application of its particular feedback circuit--the approximation of the fractional derivative and fractional integral transfer function. The transfer functions $\sqrt{s}$ and $1/\sqrt{s}$ are studied first. It is not difficult to envisage higher multiples such as $s^{\frac{1}{2}n}$ and $s^{-\frac{1}{2}n}$ for any integer n.

The block diagram of the adaptive system is reproduced in Fig. 3 with one modification--the relocation of the point from which the output is taken. The transfer function of the system as shown is

$$T(s) = \frac{1 + MB}{1 + A^2B} \cdot A \qquad (47)$$

The element which was formerly considered to be the model of the output wanted will now be the model of the square of the desired output. The feedback element is an integral control for

When simulating $1/\sqrt{s}$, use $M(s) = 1/s$ and $B(s) = B_o/s$. Then A needs to be determined.

If the feedback gain is chosen very large, the transfer function of the system when simulating $\sqrt{s}$ would be,

$$\hat{T}(s) = \lim_{B_o \to \infty} T(s) = s/A \tag{48}$$

Likewise the transfer function for simulating $1/\sqrt{s}$ is,

$$\hat{T}(s) = \lim_{B_o \to \infty} T(s) = 1/As \tag{49}$$

In order to have a transfer function of $\sqrt{s}$, it becomes necessary to choose A to be $\sqrt{s}$ in equation (48). Likewise, for a transfer function of $1/\sqrt{s}$, A would have to be $1/\sqrt{s}$ in equation (49). These values for A cannot be formed exactly, but very close approximations can be found.

To find the $\sqrt{a}$, the following equation needs to be solved for a root.

$$f(x) = x^2 - a \tag{50}$$

An approximation may be made of the smallest root by using the Newton approximation. The Newton approximation is derived as follows. Given, a function f(x) from which it is desired to determine a zero. If a point is chosen which is not a zero of f(x), it is necessary to find an estimate of the distance h from that point to the zero. That is, h must be found in

$$f(x_o + h) = 0 \tag{51}$$

The Taylor's expansion of equation (51) is,

$$0 = f(x_o) + hf'(x_o) + \frac{h^2}{2!} f''(x_o) + \frac{h^3}{3!} f'''(x_o) + \dots \tag{52}$$

The Newton approximation uses the linear approximation to the smallest root,

$$0 = f(x_o) + h\, f'(x_o) \tag{53}$$

The distance from the point chosen to the zero would be approximately

$$h = - \frac{f(x_o)}{f'(x_o)} \tag{54}$$

The first approximation to the root after the initial estimate of the root x_o would then be

$$x_1 = x_o - \frac{f(x_o)}{f'(x_o)} \tag{55}$$

The second approximation would be,

$$x_2 = x_1 - \frac{f(x_1)}{f'(x_1)} \tag{56}$$

The approximations to the root will eventually converge to the value of the root.

Lanczos (3) mentions that the method can be made to converge more rapidly if the first three terms of the Taylor expansion are used.

$$h = - \frac{f(x_o)}{f'(x_o) + h/2\, f''(x_o)} \tag{57}$$

Replacing the h in the denominator by the Newton approximation of h and then using the resulting value of h to solve for the first approximation to the root gives

$$x_1 = x_o + \frac{2\, f'(x_o)\, f(x_o)}{f(x_o)\, f''(x_o) - 2\, f'(x_o)^{\,2}} \tag{58}$$

NEWTON APPROXIMATION OF $\sqrt{s}$

The Newton method to find the first approximation to the smallest root of an equation can now be applied to equation (50) which will give an approximation to $\sqrt{s}$ if a is chosen as s.

$$x_1 = x_0 - \frac{x_0^2 - s}{2\,x_0} = \tfrac{1}{2}\,(x_0 + \frac{s}{x_0}) \tag{59}$$

The initial estimate x_0 could be chosen to be either s^0 or s^1. Either choice will give the same value for the first approximation.

$$x_1 = \tfrac{1}{2}(s + 1) \tag{60}$$

If this approximation to $\sqrt{s}$ is now used for A in the transfer function (equation 48), a first order approximation can be made to the transfer function $\sqrt{s}$.

$$\hat{T}_1(s) = \frac{s}{\frac{1}{2}(s + 1)} \tag{61}$$

This transfer function can now be simulated by the operational amplifier shown in Fig. 4. In like manner, a second order approximation can be made to the $\sqrt{s}$ by substituting the first approximation x_1 for the initial estimate x_0. The transfer function for this second order approximation would be,

$$\hat{T}_2(s) = \frac{s}{\frac{1}{2}\left[\frac{1}{2}(s + 1) + 2s/s + 1\right]} = \frac{s}{1/4 + s/4 + s/s + 1} \tag{62}$$

This transfer function can be simulated by the operational amplifier of Fig. 5.

Taking still another approximation, the transfer function by equation (63) and Fig. 6.

$$\hat{T}_3(s) = \cfrac{s}{\cfrac{1}{8} + \cfrac{s}{8} + \cfrac{s}{2(1 + s)} + \cfrac{s}{\frac{1}{2} + \cfrac{s}{2} + \cfrac{2s}{1 + s}}} \qquad (63)$$

As can be seen, the feedback impedance continues to become a more complex combination of series and parallel elements.

Figure 7 shows the frequency response of the above three transfer functions in the low-frequency range compared with the frequency response of the transfer function $\sqrt{s}$. As can be seen, the frequency response of the first approximation is a poor approximation. The amplitude rises linearly, and then rapidly approaches a constant value of two. The second order approximation has a better approximation to the frequency response of $\sqrt{s}$. This frequency response approaches a constant value of four. The third order approximation frequency response is very close to that of the $\sqrt{s}$ transfer function in the region for which the frequency response has been plotted. It can be determined from the equation that the amplitude approaches a constant value of eight instead of infinity for high frequencies. From these observations, then, it appears that the third order Newton approximation gives a good approximation to the transfer function $\sqrt{s}$ for small frequencies.

It next becomes necessary to examine the time response of the system. The response will be determined with a unit step input to see how close the simulation is. The response of the

$$E_o(s) = \hat{T}_1(s) \cdot \frac{1}{s} = \frac{2}{s + 1} \tag{64}$$

In the time domain this becomes,

$$e_o(t) = 2\, e^{-t} \tag{65}$$

As can be seen, this is an exponential with an initial value of two. The second order approximation gives the following response to a unit step input.

$$E_o(s) = \hat{T}_2(s) \cdot \frac{1}{s} = \frac{4s + 1}{s^2 + 6s + 1} \tag{66}$$

Transforming to the time domain gives the following expression for the response.

$$e_o(t) = 0.586\, e^{-0.172t} + 3.414\, e^{-5.828t} \tag{67}$$

This approximation gives an initial value of four and a response more nearly like that which is desired. The third order approximation gives a very close approximation to the response to a unit step expected from a transfer function $\sqrt{s}$. Its expression in the time domain is

$$\begin{aligned} e_o(t) = 0.259\, e^{-0.040t} + 6.569\, e^{-25.275t} \\ + 0.362\, e^{-0.447t} + 0.815\, e^{-2.240t} \end{aligned} \tag{68}$$

Other than the fact that it has an initial value of eight rather than infinity, as would be the case with the true transfer function $\sqrt{s}$, the response is nearly identical to the response expected from the transfer function $\sqrt{s}$.

Figure 8 shows these various time responses compared. The third order approximation cannot be detected from the time response of the function $\sqrt{s}$ for this scale.

NEWTON APPROXIMATION OF $1/\sqrt{s}$

By changing the system to agree with the transfer function in equation (49), the function $1/\sqrt{s}$ can also be approximated. In this case the value of A will need to be approximated by $1/\sqrt{s}$. The equation whose smallest root is to be found is

$$f(x) = x^2 - 1/s \tag{69}$$

Newton's first approximation gives,

$$x_1 = x_o - \frac{x_o{}^2 - 1/s}{2\ x_o} = \tfrac{1}{2}(x_o + \frac{1}{s\ x_o}) \tag{70}$$

The initial estimate can be chosen to be either $1/s^o$ or $1/s$. Either choice gives the same function for the first order approximation.

$$x_1 = \tfrac{1}{2}(1 + 1/s) \tag{71}$$

Since this is the first order approximation to $1/\sqrt{s}$, it can be used for the element A, thereby giving the first order approximation to the transfer function $1/\sqrt{s}$.

$$\hat{T}(s) = \frac{1}{\tfrac{1}{2}(s + 1)} \tag{72}$$

The simulating operational amplifier (Fig. 9) for this transfer function has the same feedback element as the first approximation to the transfer function $\sqrt{s}$. The input admittance, however, changes from s to 1, as shown in Fig. 9. The second order approximation using the Newton method of approximation can now be made. The transfer function is shown in equation (73), and the circuit necessary to simulate this transfer function is shown in Fig. 10.

$$\hat{T}(s) = \frac{1}{\frac{1}{4} + \frac{s}{4} + \frac{s}{s+1}} \tag{73}$$

The third approximation can be undertaken in the same manner to give a transfer function,

$$\hat{T}(s) = \frac{1}{\frac{1}{8} + \frac{s}{8} + \frac{s}{2(1+s)} + \frac{s}{\frac{1}{2} + \frac{s}{2} + \frac{2s}{1+s}}} \tag{74}$$

The operational amplifier simulation of this transfer function is seen quite readily to be as shown in Fig. 11. All three of these approximations have a transfer function which is equal to the like approximation for $\sqrt{s}$ except that it is divided by s.

The frequency response of these three Newton approximations to $1/\sqrt{s}$ are shown in Fig. 12. The first approximation has a poor approximation to the frequency response. It has a value at zero frequency of two and does not closely approximate the frequency response of $1/\sqrt{s}$ in the range of frequencies considered. The second approximation does a much better job of approximation. It likewise has a finite value at zero frequency which is four. The third approximation cannot be distinguished on the graph from the frequency response of $1/\sqrt{s}$. The only place it would differ markedly would be in the neighborhood of zero frequency. The third approximation has a value of eight at zero frequency as compared with infinite value associated with $1/\sqrt{s}$.

The impulsive response of these three approximations of

$1/\sqrt{s}$ can be seen quite readily to be the same as the response of the Newton approximations of $\sqrt{s}$ to a unit step input. These impulsive responses are shown in Fig. 8 and are expressed in equation form in equations (65), (67), and (68).

LANCZOS APPROXIMATION OF $\sqrt{s}$

The method suggested by Lanczos (3) for the solution of a root of an equation can be applied to equation (50) which will give an approximation to $\sqrt{s}$ when a is equal to s. Applying this approximation to equation (49) gives an approximation to the fractional derivative $\sqrt{s}$ which converges more rapidly than the Newton approximation.

$$x_1 = x_o \left(\frac{3\ s + x_o^2}{s + 3\ x_o^2}\right) \tag{75}$$

Again the initial estimate (x_o) can be chosen to be either s^o or s. Unlike the case using the Newton approximation, the two choices do not give identical approximations. The case where the initial estimate is equal to s^o is investigated first. This means that the first approximation to $\sqrt{s}$ will be,

$$x_1 = \frac{3\ s + 1}{s + 3} \tag{76}$$

Using this value for A in the system's transfer function, the transfer function becomes

$$\hat{T}(s) = \frac{s}{\dfrac{3\ s + 1}{s + 3}} \tag{77}$$

The associated amplifier for simulation is shown in Fig. 13. The second order approximation gives a more complex transfer function.

$$\hat{T}(s) = \frac{s}{\dfrac{3\,s + \left(\dfrac{3\,s+1}{s+3}\right)^2}{s\left(\dfrac{s+3}{3\,s+1}\right) + 3\left(\dfrac{3\,s+1}{s+3}\right)}} \tag{78}$$

The operational amplifier required for simulation (Fig. 14) is correspondingly complex.

Figure 15 shows the frequency response curves of these two approximations as compared with the frequency response of the fractional derivative $\sqrt{s}$. The second approximation cannot be distinguished from the function over the range of values plotted. From the transfer functions of the two approximations it can be seen that the frequency response does not level off at the higher frequencies as do the Newton approximations, but continues to increase as the response does for the fractional derivative function.

The time response of these two approximations to the transfer function $\sqrt{s}$ can be determined. The first order approximation gives the following output to a unit step input.

$$E_o(s) = \frac{1}{s} \times \frac{s}{\dfrac{3\,s+1}{s+3}} = \frac{s+3}{3\,s+1} \tag{79}$$

This gives equation (80) as the output expressed as a function of time.

$$e_o(t) = \frac{1}{3}\,\delta(t) + \frac{8}{9}\,e^{-1/3\ t} \tag{80}$$

The second order approximation is,

$$E_o(3) = \frac{1}{s} \times \frac{s}{\dfrac{3\ s + \left(\dfrac{3\ s + 1}{s + 3}\right)^2}{s\left(\dfrac{s + 3}{3\ s + 1}\right) + 3\left(\dfrac{3\ s + 1}{s + 3}\right)}}$$

$$= \frac{s^4 + 36\ s^3 + 126\ s^2 + 84\ s + 9}{9\ s^4 + 84\ s^3 + 126\ s^2 + 36\ s + 1} \tag{81}$$

This then gives equation (82) as the output expressed as a function of time.

$$e_o(t) = \frac{1}{9}\,\delta(t) + 0.296\ e^{-0.333t} + 0.230\ e^{-0.031t}$$
$$+ 1.900\ e^{-7.549t} + 0.538\ e^{-1.421t} \tag{82}$$

These time responses are shown in Fig. 16 compared with the time response for a transfer function of $\sqrt{s}$. Both have a delta function at zero which is not shown on these plots and which gives the approximation of the infinite value at t = 0. The second approximation to the function cannot be distinguished from the function over the range of values shown.

The same type of analysis can be followed for the approximation to $\sqrt{s}$, using s as the initial estimate. It gives a first order approximation with a transfer function as shown in equation (83) and a simulation operational amplifier as shown in Fig. 17.

$$T_1(s) = \frac{s}{s\left(\dfrac{s + 3}{1 + 3\ s}\right)} \tag{83}$$

This will immediately be recognized as being the same as the other approximation by Lanczos' method except for a different termination of the lattice network. The second approximation likewise is similar to the second approximation by Lanczos' method with an initial estimate of s^0, differing once again only by the termination. This transfer function and operational amplifier for simulation are shown in equation (84) and Fig. 18, respectively.

$$\hat{T}_2(s) = \cfrac{s}{\cfrac{3\ s + s^2\left(\cfrac{3 + s}{1 + 3\ s}\right)^2}{\left(\cfrac{1 + 3\ s}{s + 3}\right) + 3\ s\left(\cfrac{3 + s}{1 + 3\ s}\right)}}$$

$$= \frac{9\ s^4 + 84\ s^3 + 126\ s^2 + 36\ s + 1}{s^4 + 36\ s^3 + 126\ s^2 + 84\ s + 9} \tag{84}$$

Figure 19 shows the frequency response for these two approximations compared with the frequency response of the fractional derivative function. The second approximation cannot be distinguished from the function itself over the range of frequencies used except in the region of $\omega = 0$. At $\omega = 0$, the response has a value of one-third for both approximations. Also, these two approximations level off to constant amplitudes of three in the first order approximation and nine in the second order approximation.

The first order approximation gives a time response to a unit step which is shown compared with the actual function in Fig. 20. The equation for this time response is as shown below.

$$g(t) = 1/3 + 8/3\ e^{-3t} \tag{85}$$

The time response of the second approximation to a unit step input is indistinguishable from the time response of the function for the same input over the range of time shown in Fig. 20. The time response for the second approximation is

$$g(t) = \frac{1}{9} + 0.866\ e^{-3t} + 7.375\ e^{-32.258t}$$
$$+ 0.251\ e^{-0.132t} + 0.377\ e^{-0.704t} \qquad (86)$$

As can be seen from the equations, neither of these approximations goes to zero at large values of time as does the function $1/\sqrt{\pi t}$. Neither do they start at infinity.

LANCZOS APPROXIMATION OF $1/\sqrt{s}$

The function $1/\sqrt{s}$ can be approximated by using the Lanczos method of approximation, the smallest root of equation (69) giving,

$$x_1 = x_o\left(\frac{3 + s\ x_o^2}{1 + 3\ s\ x_o^2}\right) \qquad (87)$$

This approximation of $1/\sqrt{s}$ can be used as A in the transfer function shown in equation (49), and the transfer function will be an approximation to the transfer function $1/\sqrt{s}$. The initial estimate (x_o) can be chosen to be either $1/s^o$ or $1/s$. This will again give two possible simulations of the transfer function.

If the initial estimate is chosen as $1/s^o$, the first order approximation gives the transfer function,

$$\hat{T}(s) = \frac{1}{s\left(\dfrac{s + 3}{3\,s + 1}\right)} \tag{88}$$

The operational amplifier needed to simulate this transfer function is shown in Fig. 21. The second order approximation with the same initial estimate gives a transfer function as shown in equation (89).

$$\hat{T}(s) = \frac{1}{\dfrac{3\,s + s^2\left(\dfrac{s + 3}{3\,s + 1}\right)^2}{\left(\dfrac{3\,s + 1}{s + 3} + 3\left(\dfrac{s + 3}{3\,s + 1}\right)\right)}} \tag{89}$$

The simulation circuit is shown in Fig. 22.

The frequency response of these two approximations is shown compared with the frequency response for the fractional integral function in Fig. 23. Both start at infinity and decrease to zero as the function $1/\sqrt{\pi t}$ does. The frequency response of the second approximation cannot be distinguished from the frequency response of the function in Fig. 23.

The transfer functions for these two approximations of $1/\sqrt{s}$ will have an impulsive response which is the same as the response to a unit step of the Lanczos approximation to the transfer function $\sqrt{s}$ with the initial estimate chosen as s. This can readily be seen by comparing the transfer functions. The impulsive responses then can be represented by equations (85) and (86), and are graphically shown in Fig. 20.

If the initial estimate (x_0) is chosen to be 1/s, a slightly different transfer function results. The first order approximation using this initial estimate is,

$$\hat{T}(s) = \frac{s + 3}{3s + 1} \tag{90}$$

This transfer function can be simulated by an operational amplifier as shown in Fig. 24. This is recognized as being the same operational amplifier as the circuit determined with an initial estimate of $1/s^{o}$ except that it has a different termination for the lattice network. The second order approximation using the initial estimate 1/s gives a transfer function as expressed in equation (91), and requires the operational amplifier shown in Fig. 25 for simulation.

$$\hat{T}(s) = \frac{1}{\dfrac{3s + \left(\dfrac{1 + 3s}{s + 3}\right)^2}{s\left(\dfrac{s + 3}{1 + 3s}\right) + 3\left(\dfrac{1 + 3s}{s + 3}\right)}} \tag{91}$$

Figure 26 shows the frequency response of these two approximations compared with the frequency response of the fractional integral function which they approximate. The frequency response of the second order approximation cannot be distinguished from the response of the function for the scale and range of values used. It therefore gives a good approximation to the transfer function of the fractional integral.

These two approximations to $1/\sqrt{s}$ differ by a factor of 1/s from the transfer functions of the two Lanczos approximations to $\sqrt{s}$ which were formed using an initial estimate of s^{o}. The impulsive response of the two approximations to the fractional integral are therefore the same as those shown in Fig. 16. Also, the equations for the impulsive response are equation (80) for the first order approximation and equation (82) for the second order approximation.

The three methods of approximation just shown can now be compared as to their relative merit. What will be said will, in general, apply to both approximations of the fractional derivative operator and the fractional integral operator. This will be true when using the inputs which were considered for each one since the outputs were shown to be the same. The first thing that is noted is that it takes an approximation of one higher order for the Newton approximation scheme over the Lanczos approximation scheme in order to get comparable results. This is to be expected since the Lanczos method is designed to converge more rapidly.

The amplitude of the response of the fractional derivative operator to a unit step function input, $1/\sqrt{\pi t}$, starts at infinity at initial time, then drops sharply down to small values, and after two seconds approaches zero asymptotically. The Newton approximation approximates the initial infinity with an initial amplitude which is 2^n. where n is the order of the approximation. From equation (68) and Fig. 8, it can be seen that the approximate function will approach zero amplitude for large values of time at a rate comparable with function $1/\sqrt{\pi t}$ which is the desired response. The approximation using the method suggested by Lanczos with an initial estimate of s^0 for simulation of $\sqrt{s}$ and of $1/s$ for simulation of $1/\sqrt{s}$ approximates the initial infinite amplitude with a delta function. The approximation also approaches zero at a rate comparable to the actual function, as can be verified with equation (82) and Fig. 16. If the initial estimate in the Lanczos approximation is s for simulation of $\sqrt{s}$ and $1/s^0$ for simulation of $1/\sqrt{s}$, equation (86) describes the output and Fig. 20 graphically shows it. This approximation uses an initial amplitude of 3^n, where n is the order of the approximation, to simulate the initial infinite amplitude of the theoretical function. It does not approach zero but will be left with a small error which is $(1/3)^n$, where n is the order of the approximation. From the above observation it can be said that the Newton approximation and the Lanczos approximation with an initial estimate of s^0 for simulation of $\sqrt{s}$ and 1/s for simulation of $1/\sqrt{s}$ give the best results. The network for the Newton approximation is simpler, but in the next section it will be shown that the networks for both of the approximations can be reduced to nearly the same network. Figures 27 and 28 compare the three types of networks and their transfer functions for simulations of $\sqrt{s}$ and $1/\sqrt{s}$, respectively.

NETWORK THEORY IN APPROXIMATING $\sqrt{s}$ and $1/\sqrt{s}$

The appearance of the lattice networks in the above approximations brings to mind another approach to the problem of simulating fractional derivatives and fractional integrals. The characteristic admittance of a symmetrical lattice network is given by

$$Y_c = \sqrt{Y_p\ Y_q} \tag{92}$$

The admittance Y_p is the parallel arm admittance, and Y_q is the crossarm admittance. If one of these admittances is chosen to be 1 and the other s, the characteristic admittance of the network is $\sqrt{s}$. If an infinite number of these networks could be used in the feedback loop of an operational amplifier, both the fractional derivative operator and the fractional integral operator could be synthesized by making the proper choice of the input admittance. Practically an infinite number of these networks is not feasible. An approximation therefore is made by truncating the number of networks cascaded. This will give an input admittance which will be only an approximation to the characteristic admittance. Of course, the greater the number of lattice networks cascaded, the better the approximation.

The truncated group of lattice networks could be either short circuited or open circuited. These two types of terminations would give different approximations to the characteristic admittance, but as the number of networks was increased they would approach the same approximation. The short-circuited termination can be reduced quite easily to be the feedback networks found by using the Newton approximation. It requires 2^{n-1} lattice networks in series to produce a feedback admittance that is the same as the one found by the n^{th} order Newton approximation. The lattice networks will contain twice as many individual components as the networks found by using the Newton approximation, but the components will all be of the same size. All the output equations calculated are the same, and the graphs already plotted indicate the response using one, two, and four lattice networks.

If the open-circuited lattice is used for the approximation, Fig. 29 shows the circuit for simulation of the second order approximation to the fractional derivative operator, and Fig. 30 shows the simulation for a like fractional integral operator. The transfer functions for the circuits shown in Figs. 29 and 30 are given in equations (93) and (94), respectively.

$$\hat{T}(s) = \frac{s^2 + 6\,s + 1}{4\,s + 4} \tag{93}$$

$$\hat{T}(s) = \frac{s^2 + 6\,s + 1}{4\,s^2 + 4\,s} \tag{94}$$

As can be seen, the response to a unit step of the approximation to the fractional derivative is the same as the impulsive response of the approximation to the fractional integral. This is as it was before. The amplitude of the response to the above input functions is,

$$e_o(t) = 1/4\,\delta(t) + 1/4 + e^{-t} \tag{95}$$

By cascading two more networks, the feedback element would have the same number of elements as the lattice network with short-circuited termination which represents a third order Newton approximation. The transfer function for the fractional derivative approximation in this case is,

$$\hat{T}(s) = \frac{s^4 + 28\,s^3 + 70\,s^2 + 28\,s + 1}{8\,s^4 + 56\,s^2 + 56\,s + 8} \tag{96}$$

The response to a unit step input is,

$$e_o(t) = \frac{1}{8}\delta(t) + 0.125 + 0.5\,e^{-t}$$

$$+\ 1.707\,e^{-5.828t} + 0.293\,e^{-0.172e} \qquad (97)$$

Figure 31 shows these two time responses compared with the time response of the fractional derivative function. The response for the network utilizing four lattices cannot be distinguished from the response of the function for the range of values used except in the very near region of zero time. As can be seen from the equations, this approximation makes use of a delta function to simulate the initial infinite output. Also it will be noticed that the output function of the approximation will never reach zero. This disadvantage makes it slightly inferior to the approximation given by the Newton case, or, in other words, the case using the lattice with short-circuit termination.

Symmetric lattices repeatedly occur in the Lanczos approximations. The first order approximation uses a single lattice terminated either by 1 or s, depending on whether the initial estimate is chosen to be s^0 or s, respectively, for the fractional derivative, or 1/s or $1/s^0$, respectively, for the fractional integral.

The second order Lanczos approximations generate a feedback lattice with lattice elements, the feedback lattice being terminated in either 1 or s. It can be readily seen that the feedback lattice with lattice elements is equivalent to four lattices in cascade. This equivalence can be demonstrated as follows. If three of the lattice networks are taken as a four-terminal network, they can be reduced to a single lattice by using Bartlett's bisection theorem. This bisection is shown in Fig. 32.

The parallel arms of the equivalent lattice network derived by the bisection theorem have admittances which are equal to the input admittances of one-half section with the two terminals resulting from the bisection of the parallel arms shorted, and the two terminals resulting from the bisection of the crossarms open circuited. This can be seen to be the network P in the parallel arms of the lattice network in the Lanczos approximations.

The crossarm admittances of the equivalent lattice network are derived as above except that the terminals which were shorted are open circuited, and those which were open circuited are shorted. This can be seen to be the network Q in the crossarms of the lattice network as used in the Lanczos approximations. Three cascaded lattices then replace the single lattice with lattice elements in the feedback element of the operational amplifier.

The termination of this complicated lattice network in each Lanczos case is another lattice network with the same elements as the three cascaded lattice networks, and with a termination admittance of either 1 or s. The total feedback network in the Lanczos approximation is the equivalent to four cascaded lattices terminated in an admittance of either 1 or s. This group of lattices is seen to be of the same type as for the Newton approximation from above, and of the same length for comparable degrees of approximation. As was seen when discussing the Lanczos approximations, the networks which would give the lattices terminated in an element of 1 gave a slightly better approximation since these give time responses in the input functions chosen which do attain an amplitude of zero at large values of time.

The results of the above work with simulation of the operators $\sqrt{s}$ and $1/\sqrt{s}$ can be extended to all fractional powers of s that are integral powers of 1/2. The $\sqrt[4]{s}$ operator can be approximated by substituting the lattice networks which have an approximate characteristic admittance of $\sqrt{s}$ in the parallel arms of another lattice which has crossarm admittance of 1, as shown in Fig. 33 for a first approximation to $\sqrt[4]{s}$ of the Newton type. This total feedback network could then be applied as the parallel arms of another lattice network and the whole thing used as a feedback element to simulate $\sqrt[8]{s}$. As can be seen, this rapidly develops into some very complex networks which are not easily reduced.

APPLICATIONS OF FRACTIONAL OPERATORS

The operator $\sqrt{s}$ appears in several types of problems. One of these is the solution of an RC transmission line as was shown by Heaviside (2). The circuits considered could be used to simulate such a line.

The equations of heat flow can be simulated by a series of RC networks, and the equation describing such flow therefore contains a fractional operator. In analog simulations of these heat flow problems, long series of RC networks have been used

(4). The use of the above operational amplifier and lattice network would greatly simplify the analog simulation of these problems, and would require less equipment.

Another problem quite similar to the heat problem would be the diffusion of neutrons in a nuclear reactor. Any problem then that could be simulated with an RC line could possibly better be simulated by the operator $\sqrt{s}$ and the simulation schemes shown.

Another application of the transfer function $1/\sqrt{s}$ occurs in the compensation of servos. The usual criterion of goodness of a servo's response to a unit step function is zero steady-state error. The canonical form for this criterion is shown in Fig. 34. This canonical form will be referred to as canonical form I and has a response to a unit step input of

$$g(t) = 1 - e^{-kt} \tag{98}$$

If the criterion of goodness of a servo's response to a unit step function is zero steady-state error and large initial slope, then the canonical form is shown in Fig. 35. This will be called canonical form II. The transfer function of the servo is

$$T(s) = \frac{k}{\sqrt{s} + k} \tag{99}$$

If a unit step is the input signal, the output is

$$g(t) = 1 - e^{k^2 t} + e^{k^2 t} \operatorname{erf} k\sqrt{t} \tag{100}$$

The response is shown in Fig. 36 for both canonical form I and canonical form II with gains, K, of one and two. As can be seen from the response functions, the servo of canonical form II will have zero steady-state error. It has a faster rise time than the servo of canonical form I; however, after the initial quick rise it approaches zero steady-state error at a slower rate than canonical form I.

The frequency responses of these two canonical forms are shown for gains of one and ten in Figs. 37 and 38, respectively. The response of canonical form II improves more with changes to higher gain than does canonical form I. Its low-frequency response still is not as good, however, meaning that canonical form II will still take a longer time to read zero steady-state error.

For a position servo which has high damping, the system compensated with the fractional derivative operator is as shown in Fig. 39. The transfer function will be,

$$T(s) = \frac{K}{Js^{3/2} + Rs^{\frac{1}{2}} + K} \tag{101}$$

With a unit step input the time response could be solved from the following equation.

$$g(t) = e^{-2At/3}\mathcal{L}^{-1}\left[\frac{(s + A/3) - 1}{\sqrt{s - \frac{2A}{3}}\left[s^3 - \frac{A^2}{3}s - \left(\frac{2A^3 + 27}{27}\right)\right]}\right] \tag{102}$$

where $A = \frac{R}{\sqrt[3]{JK^2}}$. The equation is not readily solvable as a function of time in closed form. The second term in the denominator has one real root and two complex conjugate roots if $\frac{b^2}{4} + \frac{a^3}{27} > 0$, where $b = \left(\frac{26\ A^2 - 27}{27}\right)$ and $a = -\frac{A^2}{3}$. It has three real roots for $\frac{b^2}{4} + \frac{a^3}{27} \leq 0$. The condition which separates the complex roots from the real roots is $\frac{b^2}{4} + \frac{a^3}{27} = 0$. It is found that two complex roots exist for all values of A except when $A < -1.89$. In a physical system A cannot be negative; therefore no values can be chosen for the parameters J, R, and K for which there are no complex conjugate terms. The actual time response of a system of this type will be shown in an analog computer simulation later.

A position servo with low damping and fractional derivative compensation has approximately the form as shown in Fig. 40. The transfer function is,

$$T(s) = \frac{K}{s^{3/2} + K} \tag{103}$$

The response to a unit step input can be expressed as,

$$g(t) = 1 - \frac{e^{\alpha t}}{3} + \frac{e^{\alpha t}}{3} \operatorname{erf} \sqrt{\alpha t} - \frac{2\, e^{-\alpha/2\, t}}{3} \cos \frac{\sqrt{3}\,\alpha}{2} t - 2\, e^{-\alpha/2\, t} \int_0^t \frac{1}{\sqrt{\pi t}}\, e^{\alpha/2\, t} \sin\left[\frac{\sqrt{3}\,\alpha}{2}(t - \tau) + \frac{5\pi}{6}\right] d\tau \tag{104}$$

The last integral can be evaluated only by numerical methods. In lieu of this, an analog computer simulation of the approximation is shown in the next section.

COMPUTER SIMULATIONS

The lattices required to simulate the fractional operators were built and analog computer simulations were made of the approximate fractional operators. The feedback element used consisted of five cascaded lattices. All four terminations which are indicated in the preceding material were tried. Figure 41 shows the response of the approximate fractional derivative operator to a unit step input. No difference can be detected for any of the four different terminations over the time range used. The response is the same as the expected one, giving a very good approximation to the fractional derivative operator except at the initial time.

Figure 42 shows the response of the approximation to the fractional integral operator to a unit step input. Again the response is the same for all of the terminations, and over the range of time shown closely approximates to expected response of a fractional integral.

Analog computer simulations were also made for the servo compensation techniques indicated in the preceding section. Associated with each of the curves shown is a diagram of the servo simulated. Figures 43 and 44 show the response to a unit step input of servos of canonical form I and canonical form II, respectively. The curves are as predicted by the response equation, the plot of which is shown in Fig. 36. Figures 45 through 47 show the response of a position servo without compensation. The three curves are for three different values of damping. The next three figures, Figs. 48 through 50, show these same servos with fractional derivative compensation. This compensation definitely does give a much quicker initial slope than the uncompensated servo. Also for the servos with less damping, the initial oscillations are all but eliminated. There is only one overshoot at the higher gains. The fractional derivative compensation does have a disadvantage, though, which is particularly noticeable in the servos with higher damping. This disadvantage is that after the initial large slope, the servo approaches the steady-state value at a slow rate.

The fact that the fractional derivative compensated servo and the servo with no compensation are each strong where the other one is weak suggests using a compensation technique which is an average of these two. A particular average transfer function which will give the greatest weight to the function with the largest value is,

$$T(s) = \frac{(1)^2 + (\sqrt{s})^2}{1 + \sqrt{s}} = \frac{1 + 1/s}{1/\sqrt{s} + 1/s} \tag{105}$$

The forward loop transfer function of the servo is then,

$$\begin{aligned} T(s) &= \left(\frac{1 + 1/s}{1/\sqrt{s} + 1/s}\right) \left[\frac{K}{s(Js + R)}\right] \\ &= \left[\frac{1 + 1/s}{1 + \sqrt{s}}\right] \left[\frac{K}{Js + R}\right] \end{aligned} \tag{106}$$

Figure 51 shows the response to a unit step input of the averaging transfer function which has replaced the integral function. Also shown in Fig. 51 is the response of the integral function to a unit step input. It can be seen that there is an initial jump and that the rate after this jump is higher than the integral function. Figures 52 through 54 show the response to a unit step input of the same position servo considered previously, using this average transfer function for compensation. This combination combines the good points of both compensation techniques, giving a high initial slope, eliminating the oscillation, and still reaching steady-state conditions quickly.

Figure 55 shows the analog simulation of the response of the approximate form of a position servo with low damping and fractional derivative compensation which was considered earlier. The servo has only one overshoot which is approximately the same amplitude for all values of gain. The response is therefore similar for all values of gain except for changes in initial rise time. The servo response for smaller values of damping is shown in Figs. 56 and 57. As low values of damping are approached, high gains give an oscillatory behavior. With a damping factor of two, as shown in Fig. 56, the servo goes into oscillations which increase in magnitude with time if a gain of ten is used. This method of compensation of a position servo produces no beneficial results, but instead makes the servo unstable at high gains.

Figure 58 shows the analog simulation of a velocity servo with fractional integral control. A ramp input was used to determine if the servo would be able to follow with zero velocity lag. As can be seen from the curves, even at nine seconds the velocity lag of the servo was still increasing. Fractional integral compensation is not helpful, therefore, in eliminating velocity lag. The average transfer function between integral compensation and fractional integral compensation was also tried for the velocity servo. Figure 59 shows these results. As expected, the velocity lag is still there. The servo with self average of 1 and $\sqrt{s}$ comes to its final value of lag more quickly than the servo with fractional integral compensation.

CONCLUSIONS

Approximations to the fractional operators $1/\sqrt{s}$ and $\sqrt{s}$ are made by using the Newton and Lanczos approximation techniques. These approximations are readily applied to operational amplifier circuits for simulation. The networks developed for the feedback loop of these operational amplifiers consist of cascaded lattice networks with resistors and capacitors. The characteristic admittance of these lattices is $\sqrt{s}$. Therefore in the limiting case of infinite number of lattices in cascade, the functions $\sqrt{s}$ and $1/\sqrt{s}$ would be simulated. Both approximate functions are simulated by truncating the number of lattices in cascade.

The fractional operators can be used in several different applications. They can be used in the analog simulation of heat transfer problems and neutron diffusion problems. Also they may find an application as compensation for servos. In this application, the fractional derivative compensation of a position servo gives a higher initial slope than the uncompensated servo has, eliminates most of the oscillation in servos with a low damping factor, and has zero steady-state error. Fractional derivative compensation has the disadvantage of giving a slower approach to the steady-state condition after its initial high slope, than does the uncompensated servo. A better result is obtained by using a self average of the fractional derivative and the identity transfer functions. This average incorporated the good points of each.

The fractional integral compensation of a velocity servo gives no help in the elimination of velocity lag. In fact, with fractional integral compensation the velocity lag is slow to even attain a steady-state value. The self average of integral compensation and fractional integral compensation also gives a steady-state velocity lag though it attains steady-state conditions much quicker than the servo with fractional integral compensation only.

ACKNOWLEDGMENT

The author wishes to express his appreciation to Dr. C. A. Halijak, his major instructor, for the ideas and helpful suggestions so generously given in the preparation of this paper.

REFERENCES

1. Campbell, Graham.
   Use of an adaptive servo to obtain optimum airplane response. Cornell Aeronautical Laboratory Report C.A.L. 84. Buffalo, N.Y.: Cornell Aeronautical Laboratory, Inc., 1957.

2. Heaviside, Oliver.
   Electromagnetic theory. New York: Dover Publications, Inc., 1950.

3. Lanczos, Cornelius.
   Applied analysis. Englewood Cliffs, N.J.: Prentice-Hall, Inc., 1956.

4. Wright, W. L. and C. A. Booker.
   How analog networks solve air-conditioning problems. Electronics, 32(52):34-37. December 25, 1959.

APPENDIX

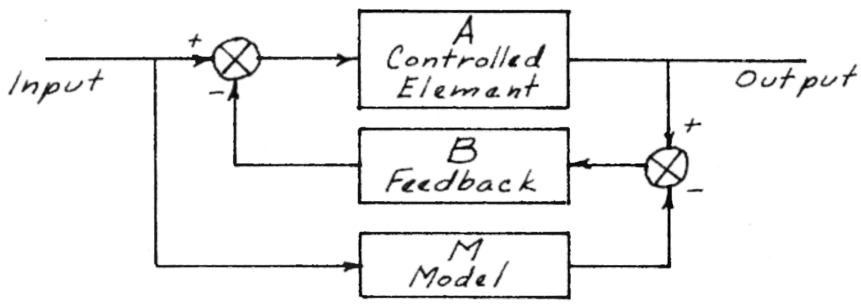

Fig. 1. Block diagram of the linear adaptive servo.

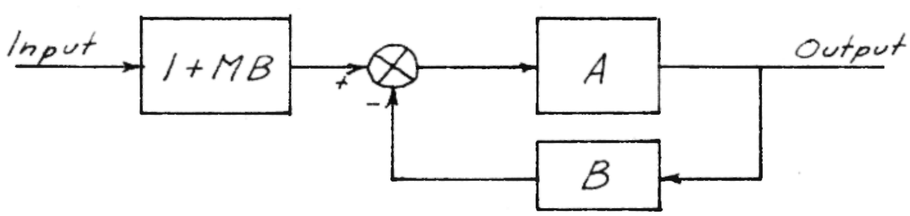

Fig. 2. Reduced block diagram of the linear adaptive servo.

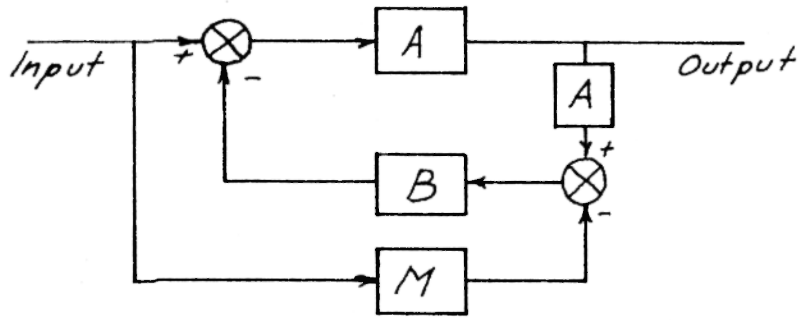

Fig. 3. Block diagram of linear adaptive servo modified for simulating $\sqrt{s}$ transfer function.

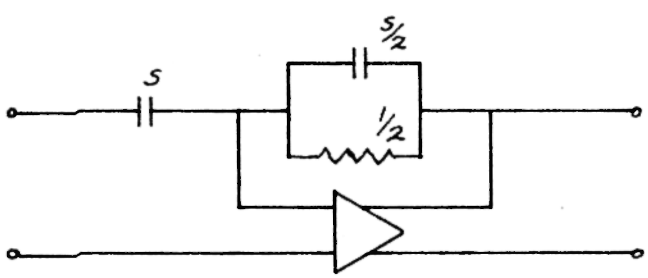

Fig. 4. Operational amplifier for first order Newton approximation of $\sqrt{s}$.

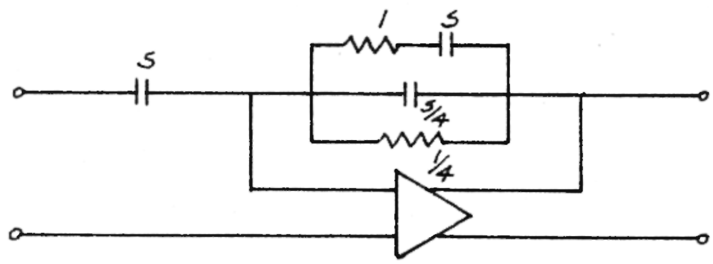

Fig. 5. Operational amplifier for second order Newton approximation of $\sqrt{s}$.

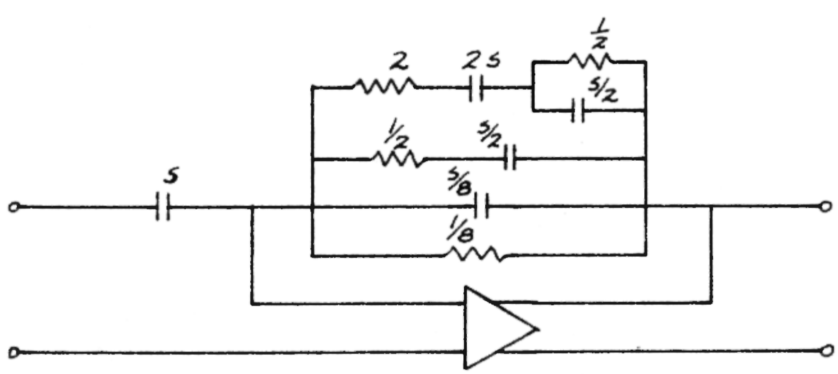

Fig. 6. Operational amplifier for third order Newton approximation of $\sqrt{s}$.

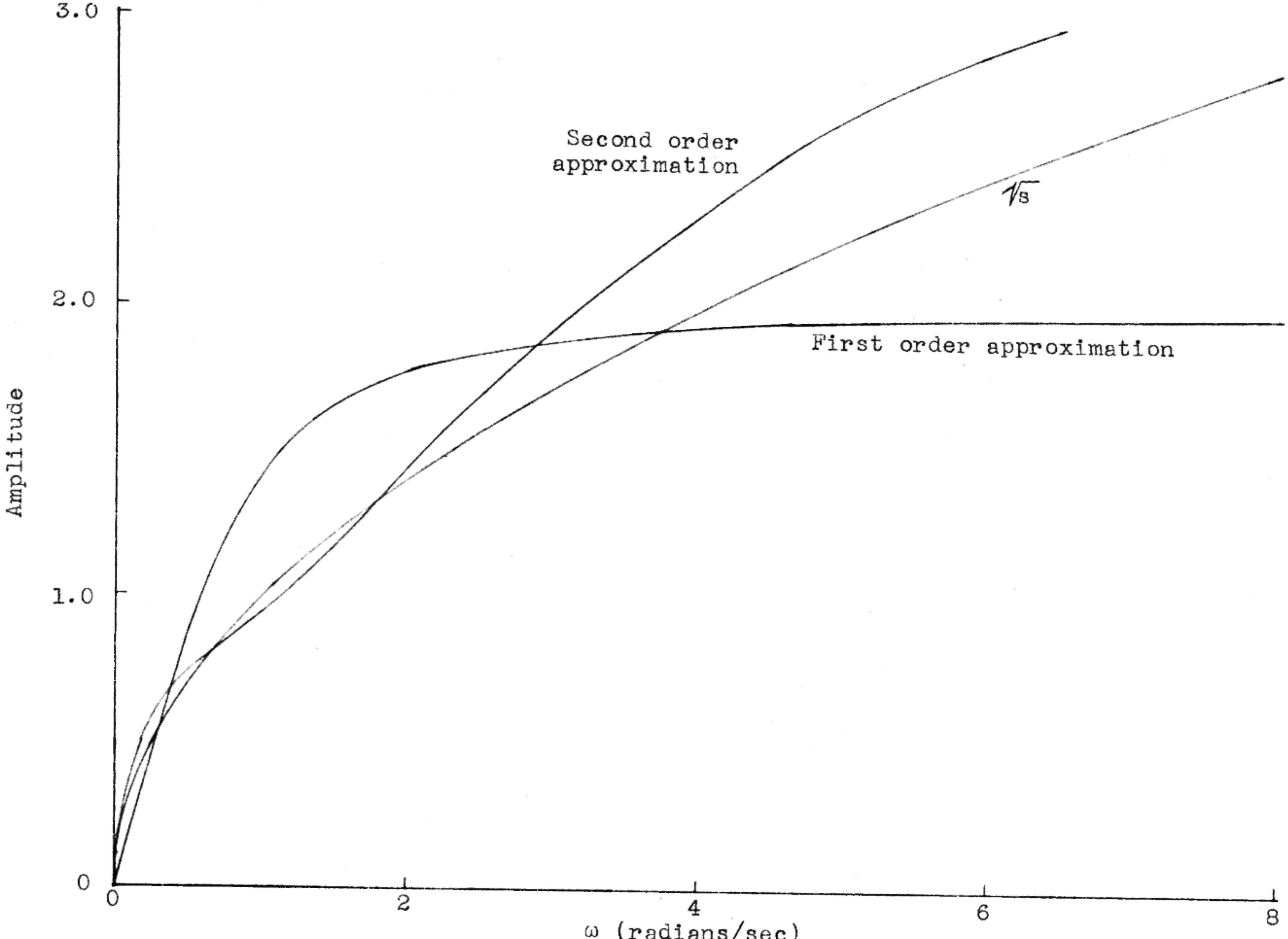

Fig. 7. Frequency response of Newton's approximation to s.

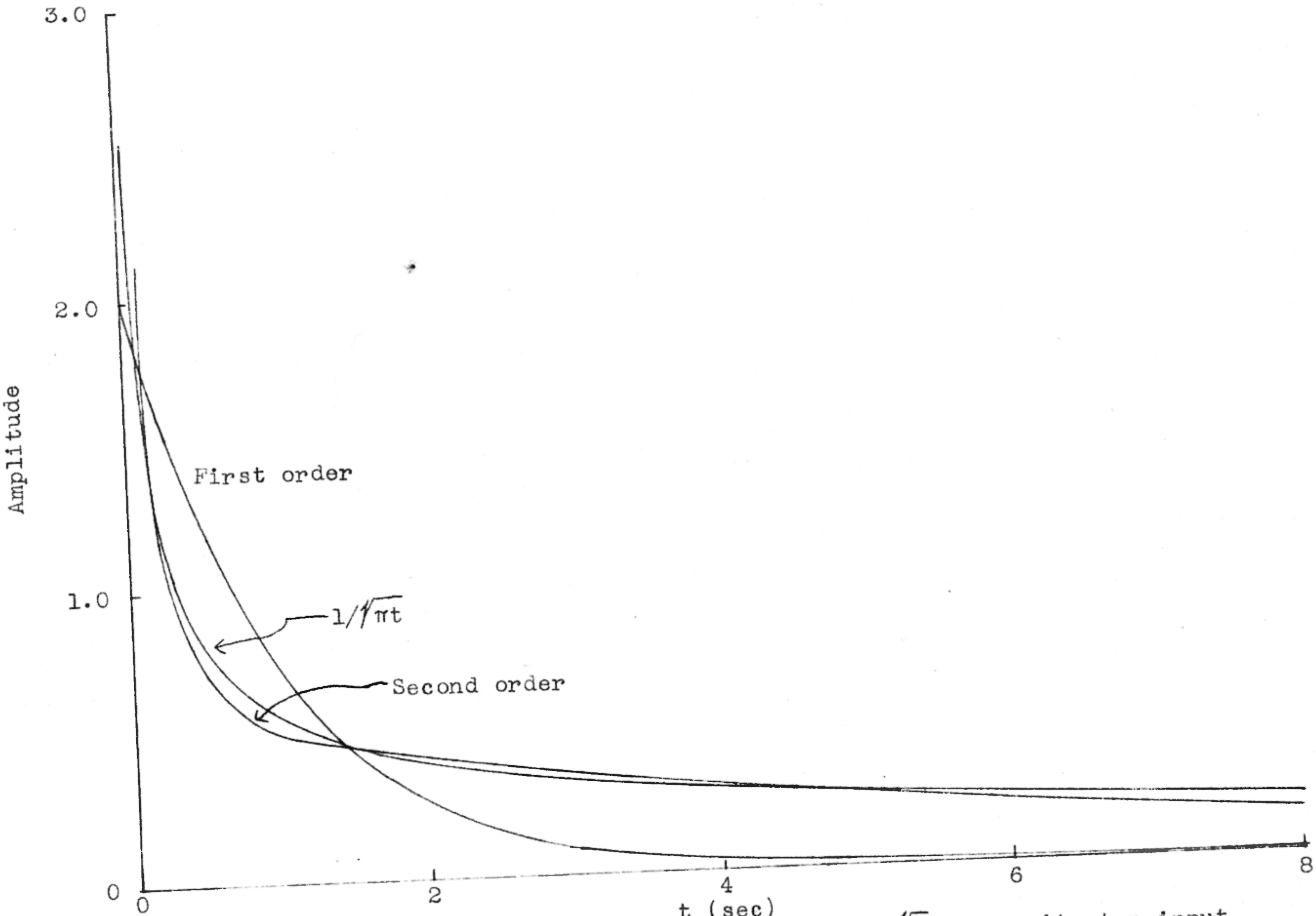

Fig. 8. Response of Newton's approximation of $\sqrt{s}$ to a unit step input.

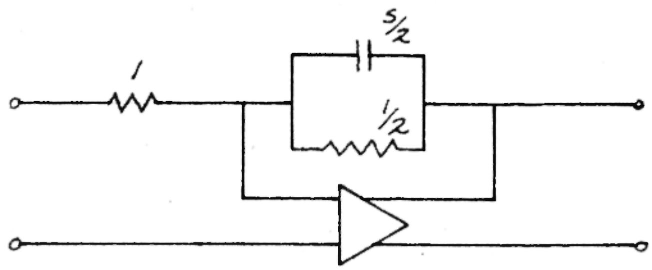

Fig. 9. Operational amplifier for first order Newton approximation of $1/\sqrt{s}$.

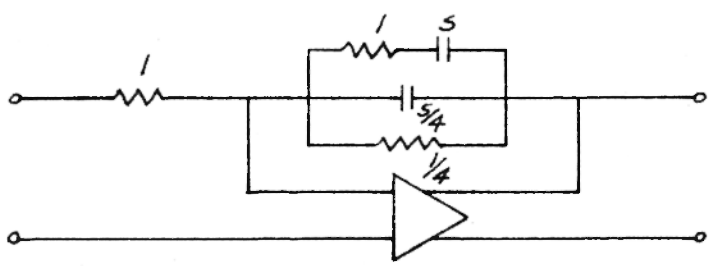

Fig. 10. Operational amplifier for second order Newton approximation of $1/\sqrt{s}$.

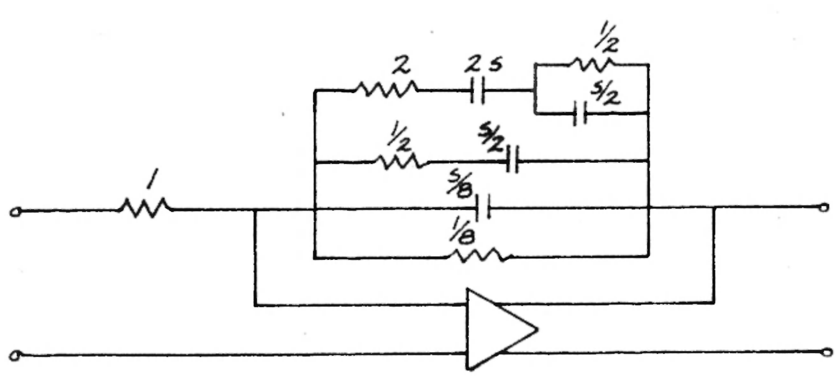

Fig. 11. Operational amplifier for third order Newton approximation of $1/\sqrt{s}$.

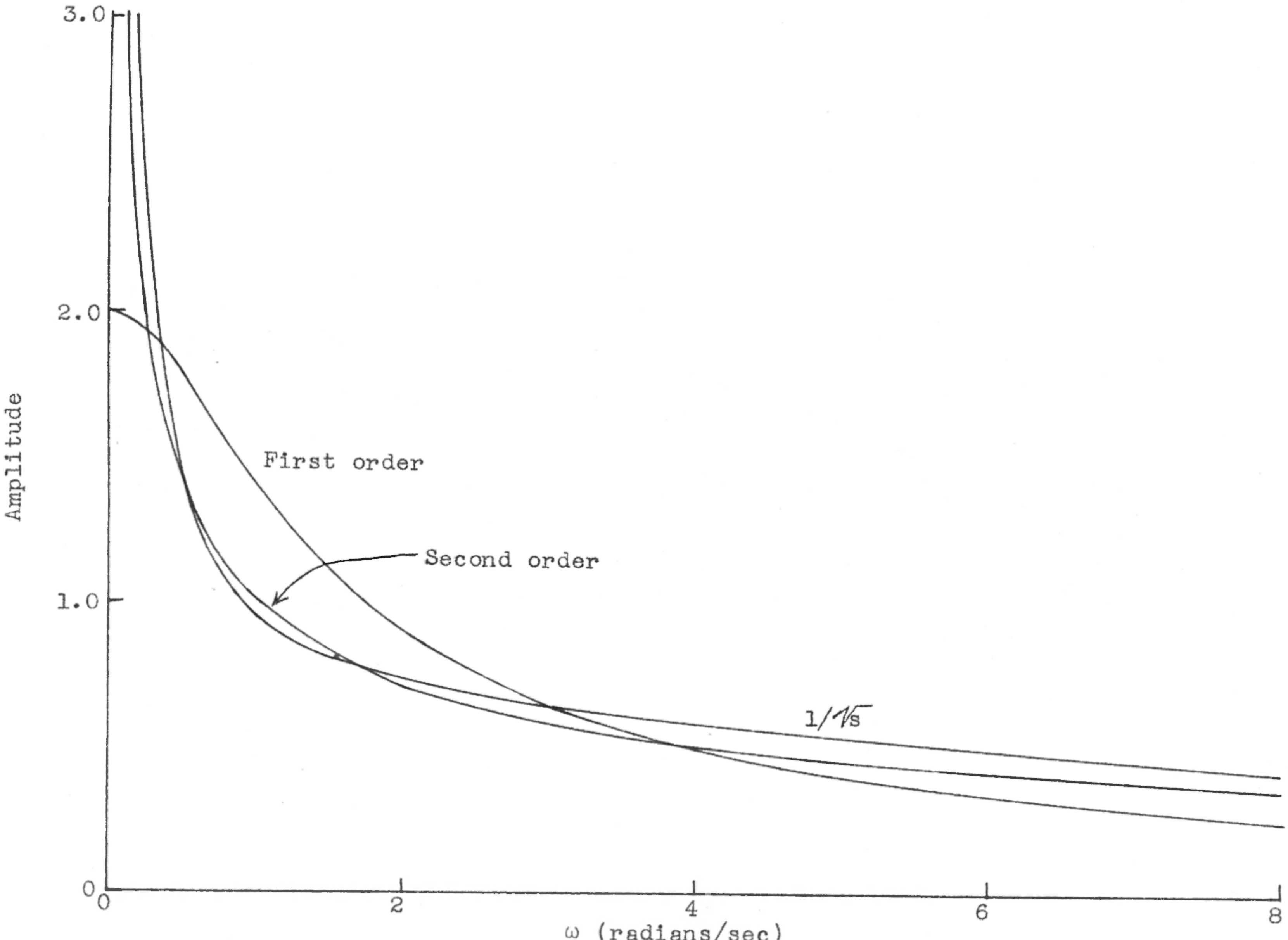

Fig. 12. Frequency response of Newton's approximation of $1/\sqrt{s}$.

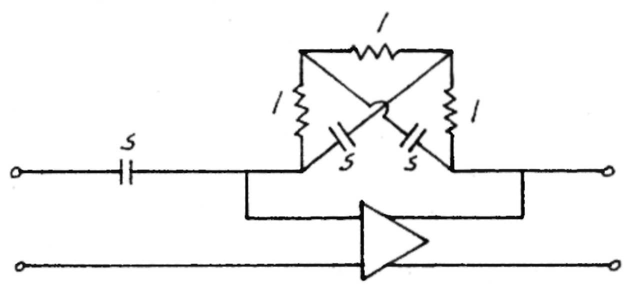

Fig. 13. Operational amplifier for first order Lanczos approximation of $\sqrt{s}$ with initial estimate s^0.

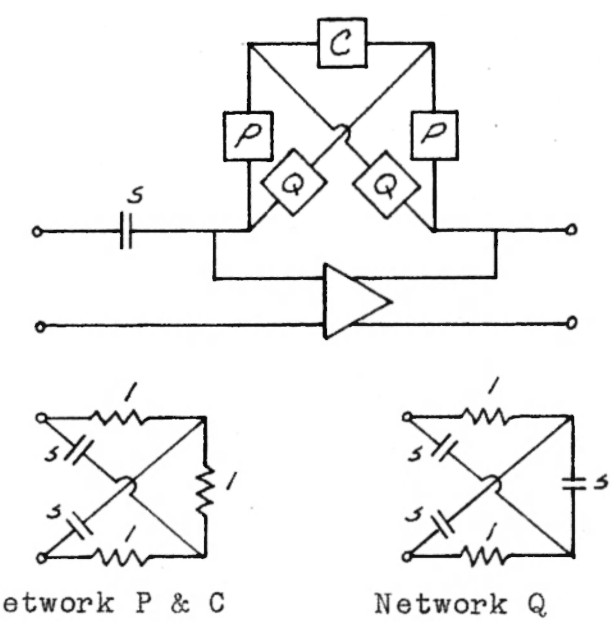

Fig. 14. Operational amplifier for second order Lanczos approximation of $\sqrt{s}$ with initial estimate s^0.

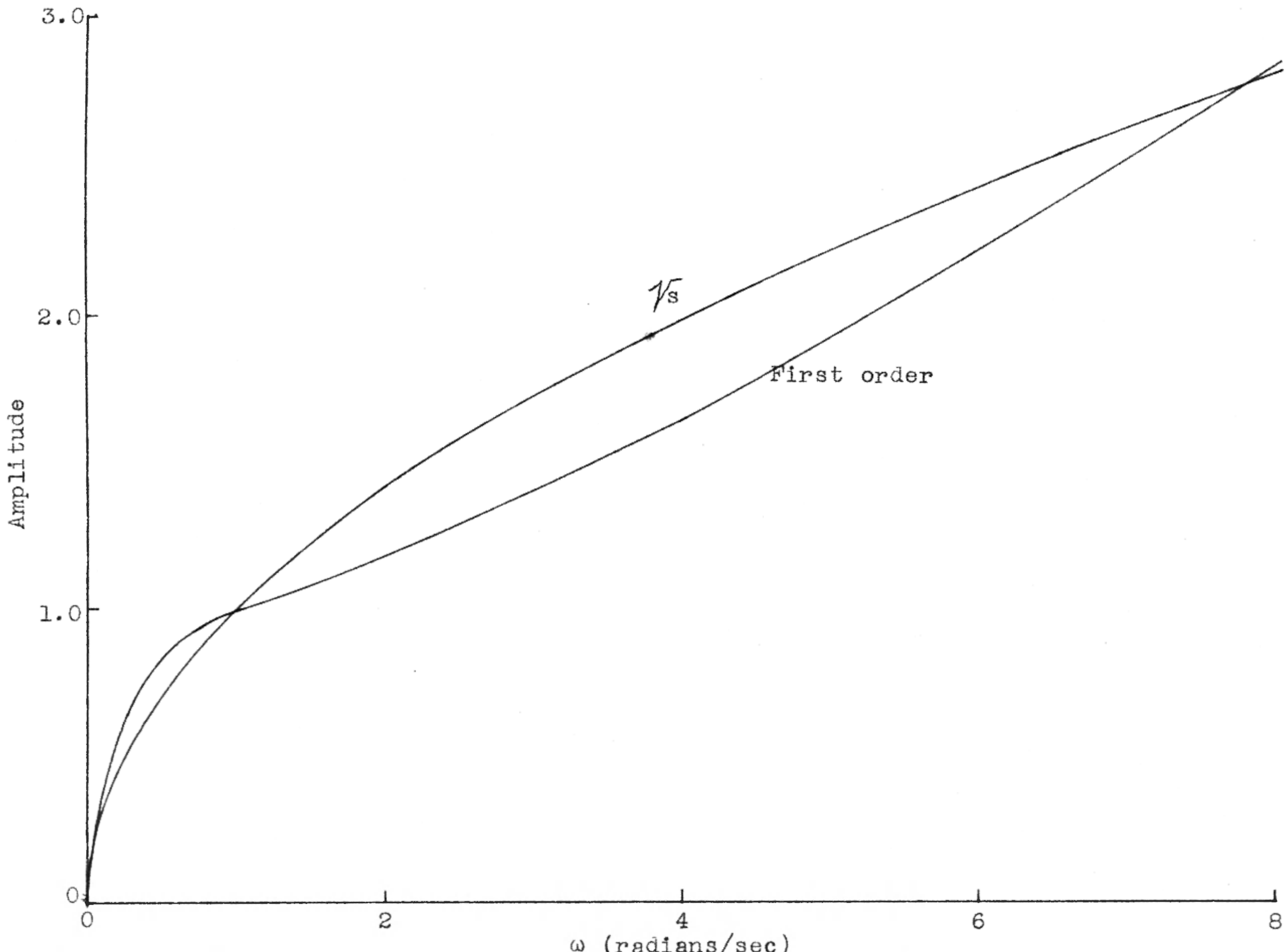

Fig. 15. Frequency response of Lanczos approximation of $\sqrt{s}$ with initial estimate s^0.

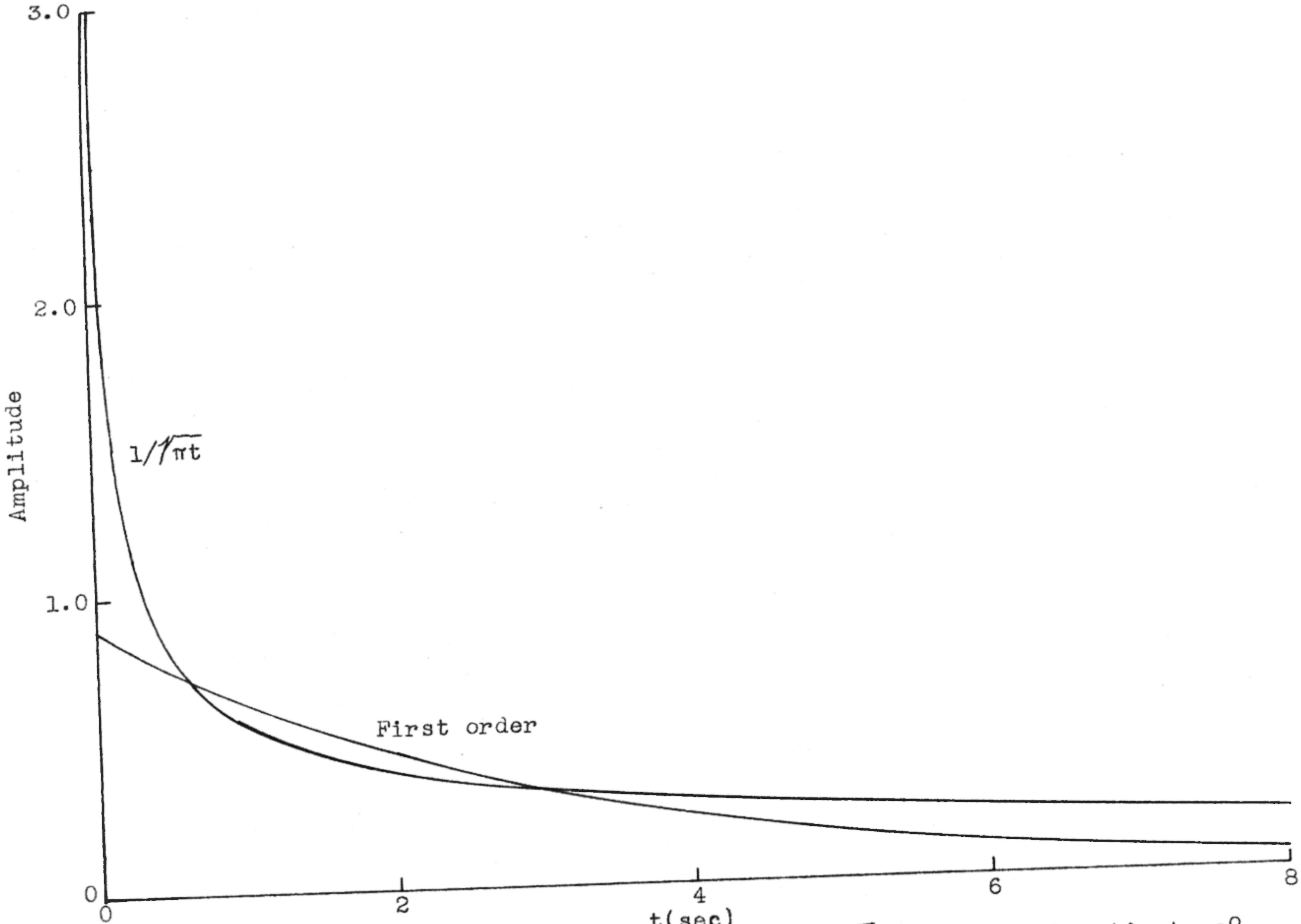

Fig. 16. Response of Lanczos approximation of $\sqrt{s}$ with initial estimate s^{o}

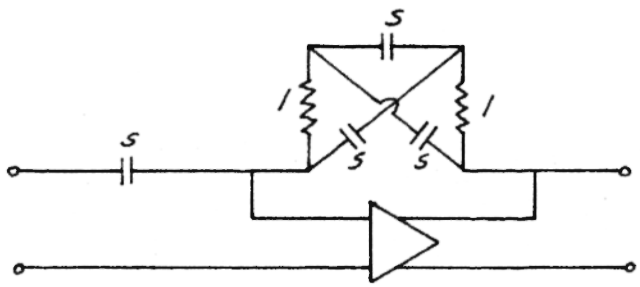

Fig. 17. Operational amplifier for first order Lanczos approximation of $\sqrt{s}$ with initial estimate s.

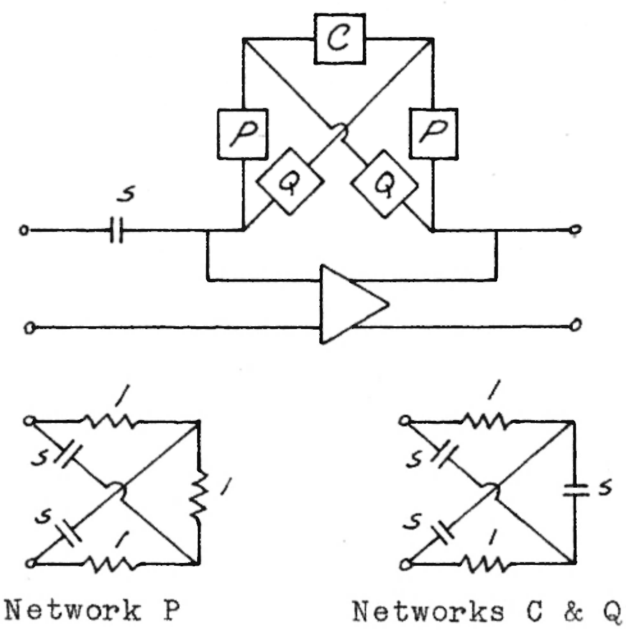

Fig. 18. Operational amplifier for second order Lanczos approximation of $\sqrt{s}$ with initial estimate s.

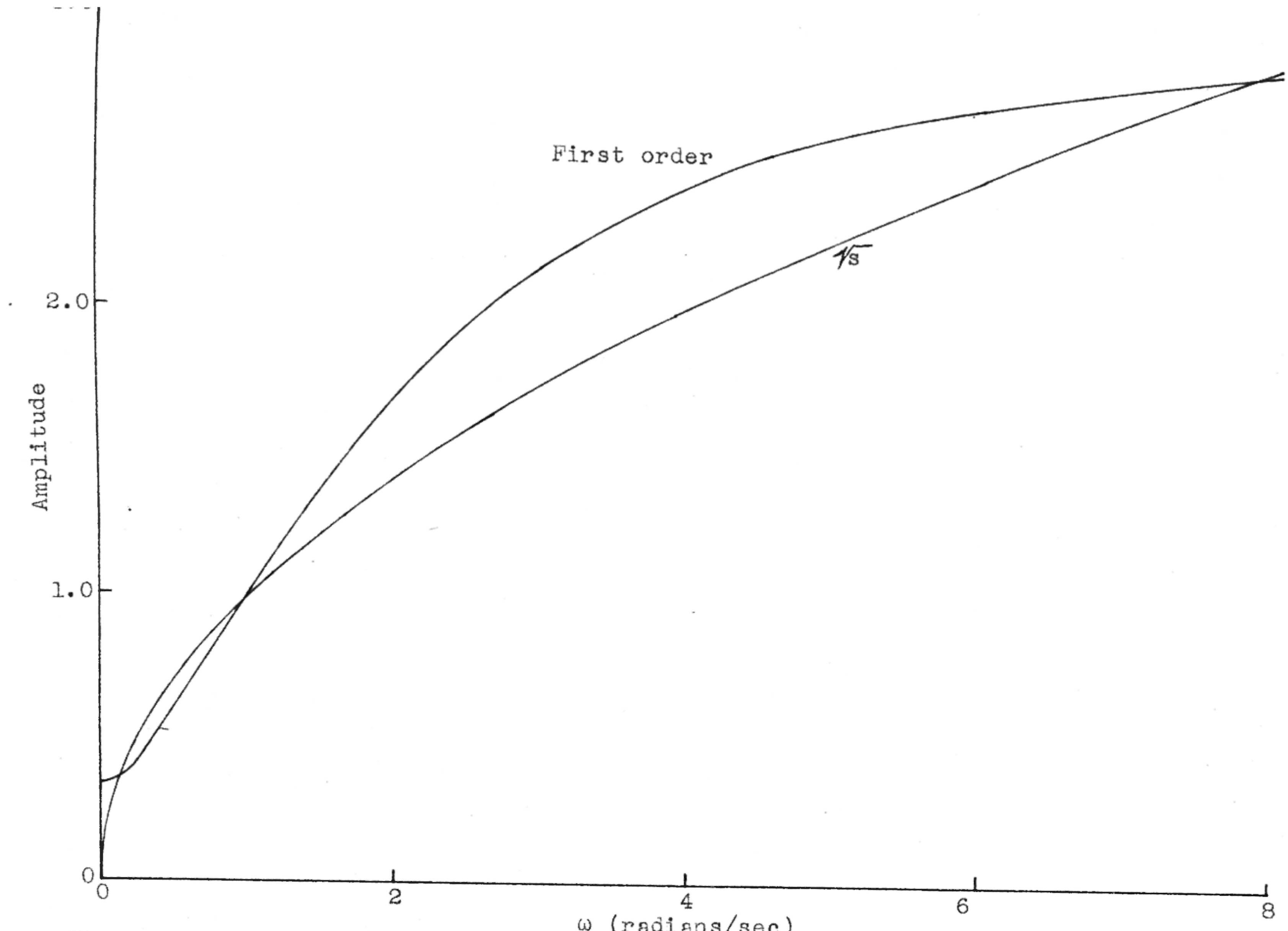

Fig. 19. Frequency response of Lanczos approximation of $\sqrt{s}$ with initial estimate s.

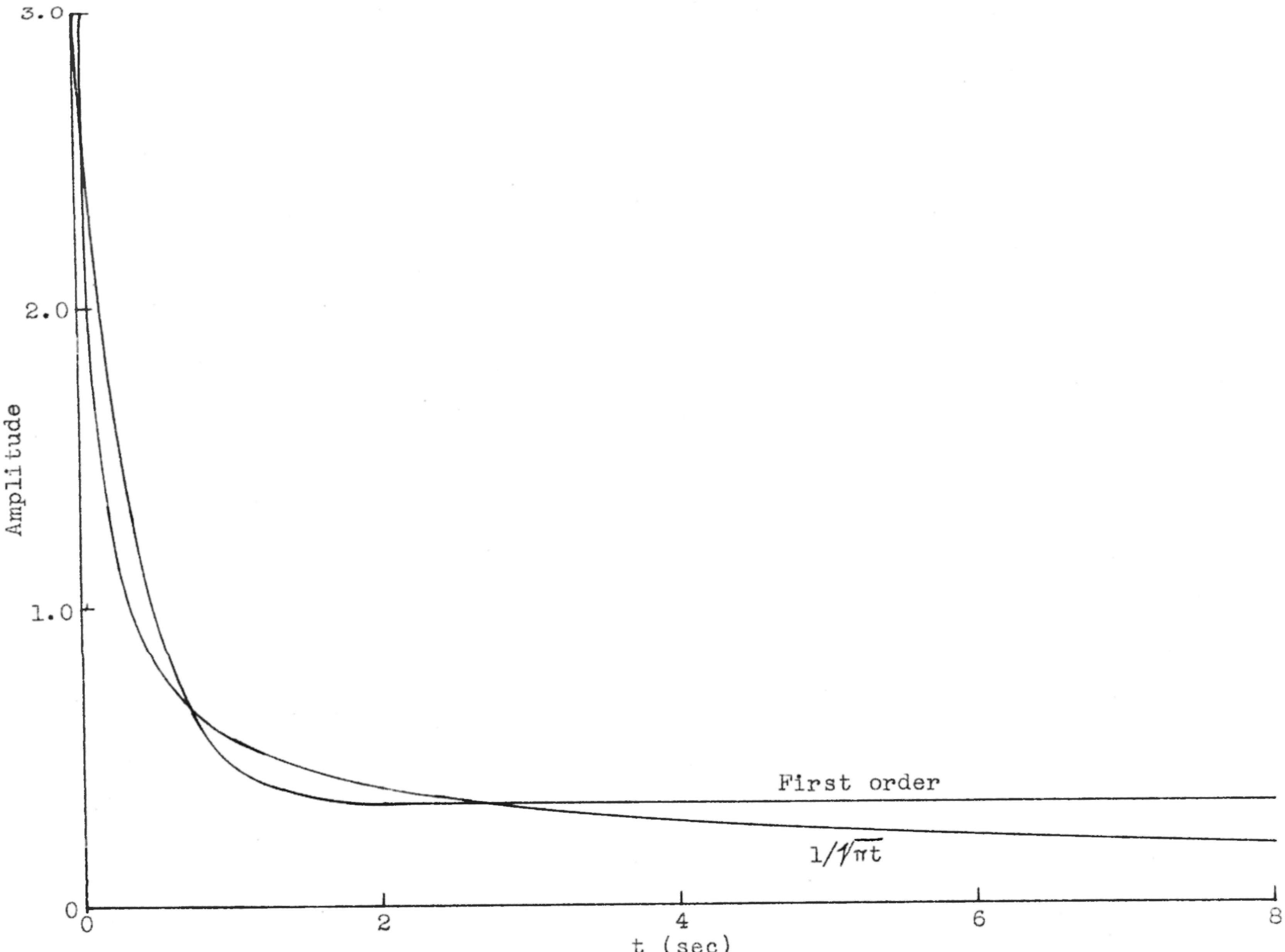

Fig. 20. Response of Lanczos approximation of $\sqrt{s}$ with initial estimate

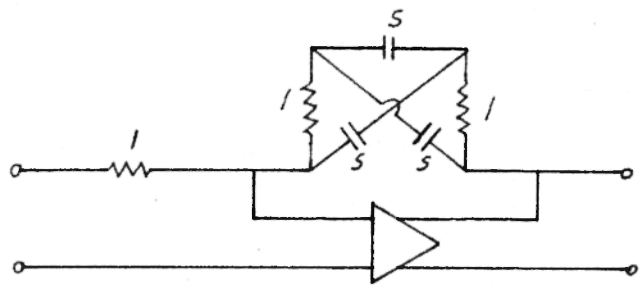

Fig. 21. Operational amplifier for first order Lanczos approximation of $1/\sqrt{s}$ with initial estimate s^0.

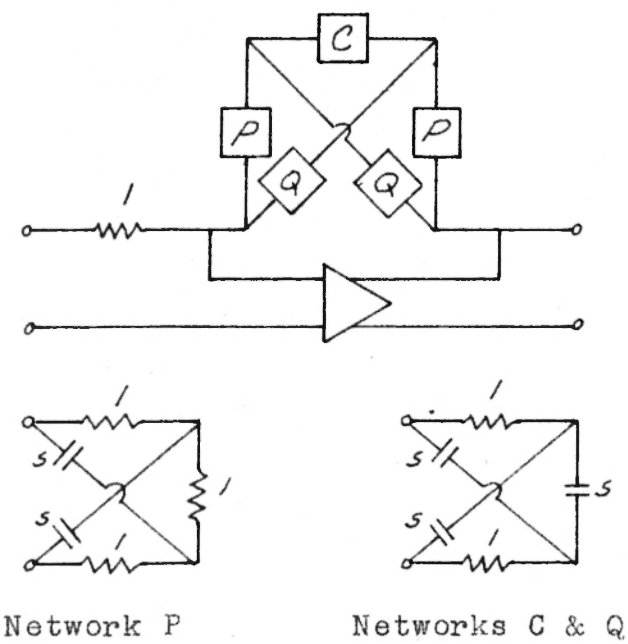

Fig. 22. Operational amplifier for second order Lanczos approximation of $1/\sqrt{s}$ with initial estimate s^0.

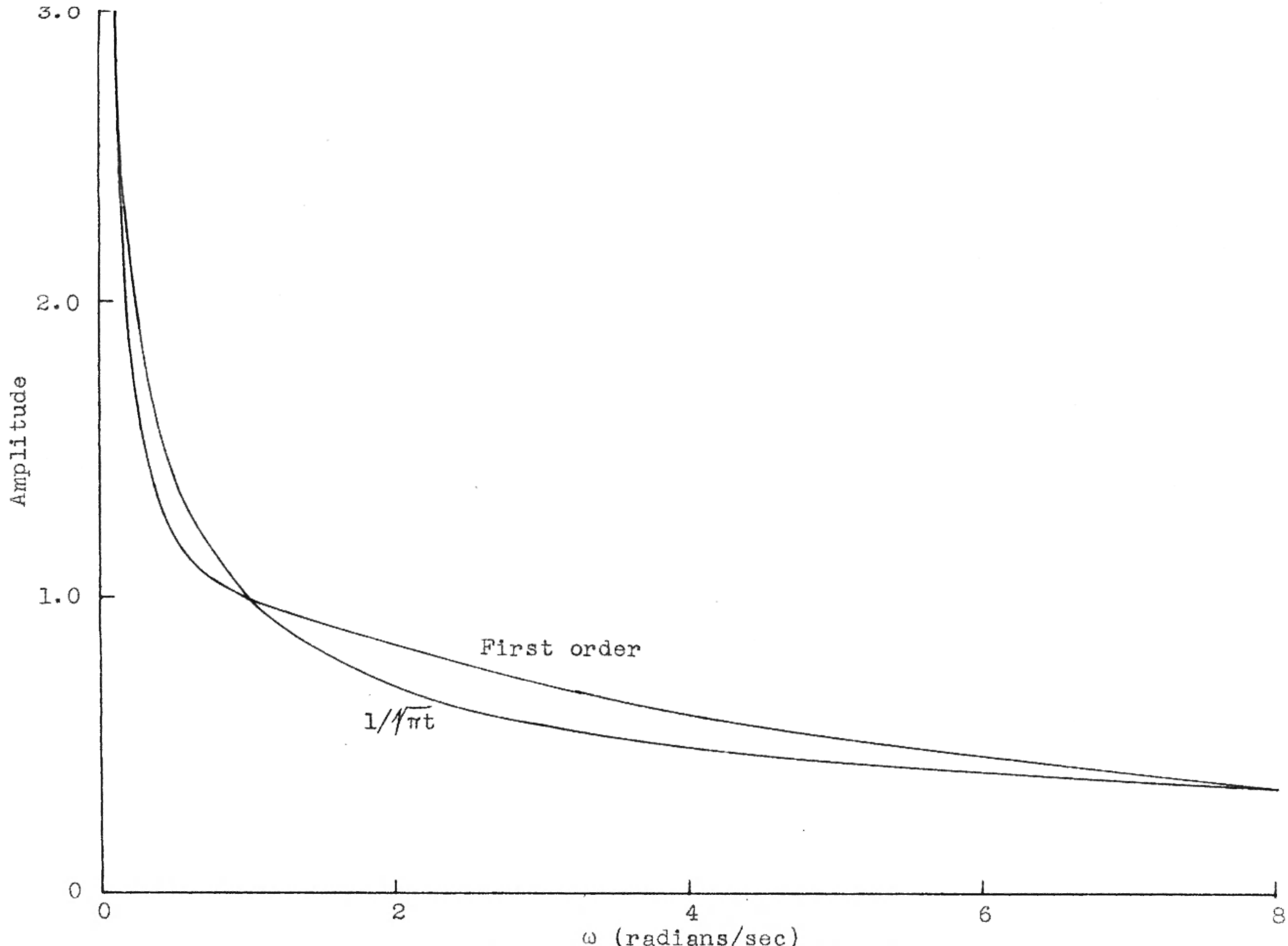

Fig. 23. Frequency response of Lanczos approximation of $1/\sqrt{s}$ with

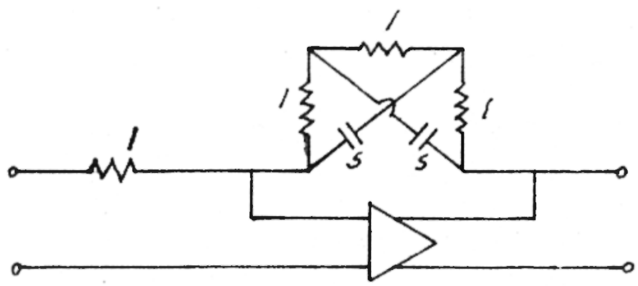

Fig. 24. Operational amplifier for first order Lanczos approximation of $1/\sqrt{s}$ with initial estimate $1/s$.

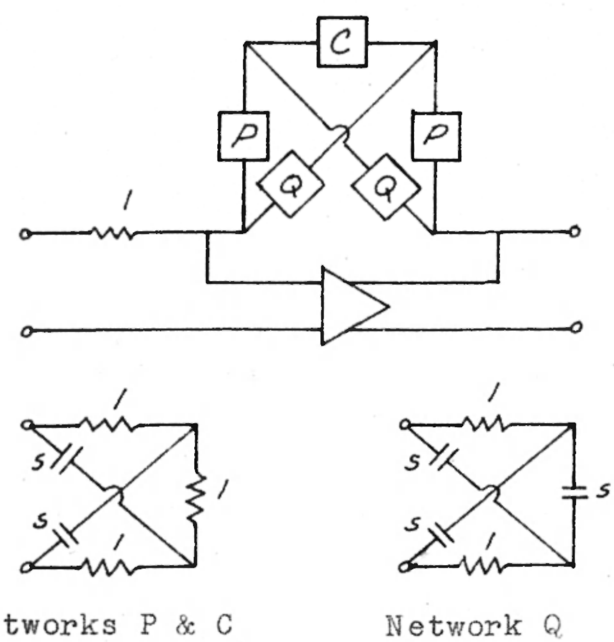

Fig. 25. Operational amplifier for second order Lanczos approximation of $1/\sqrt{s}$ with initial estimate $1/s$.

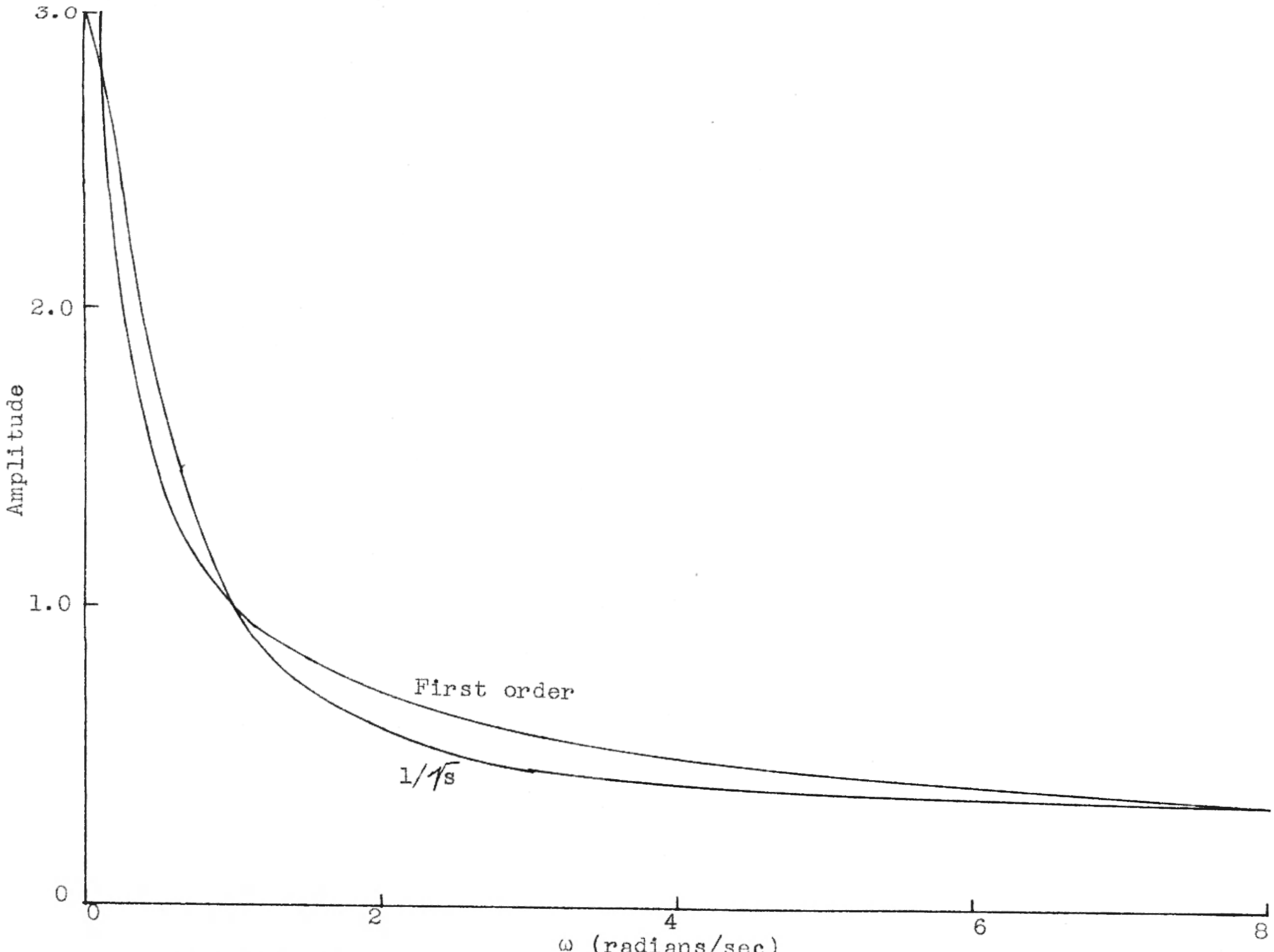

Fig. 26. Frequency response of Lanczos approximation of 1/√s with

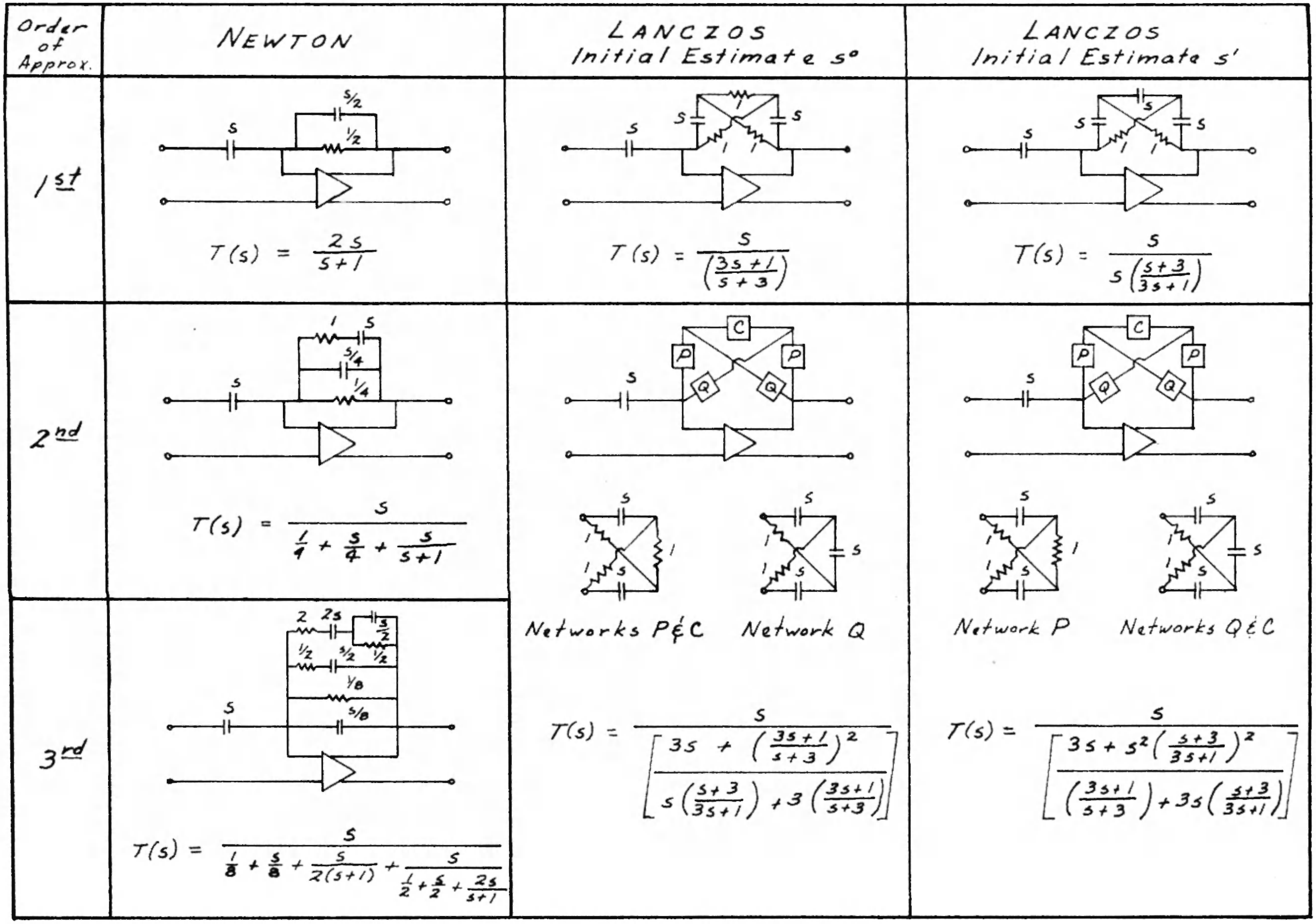

Fig. 27. Comparison of operational amplifiers for the approximations of $\sqrt{s}$.

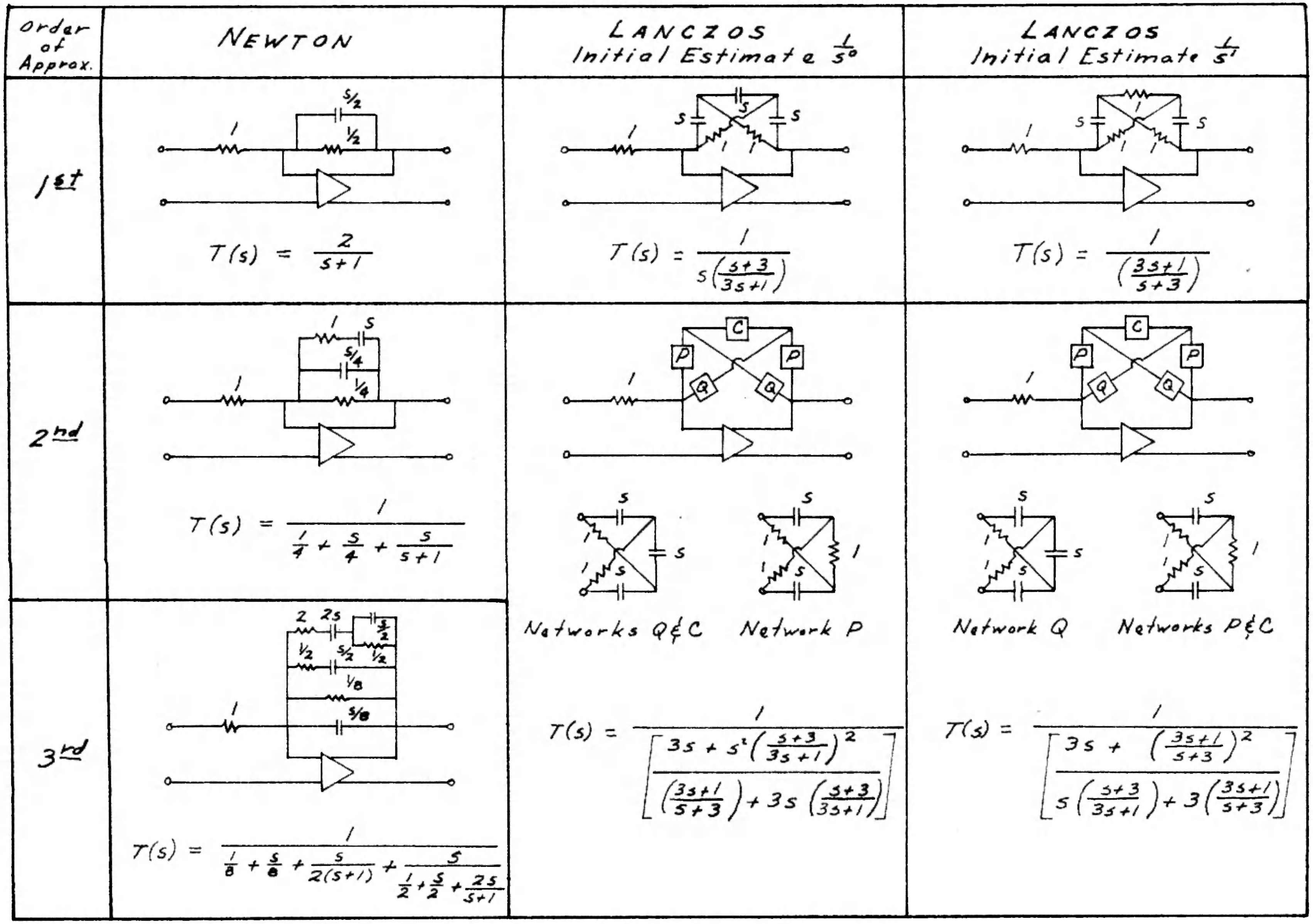

Fig. 28. Comparison of operational amplifiers for the approximations of $1/\sqrt{s}$.

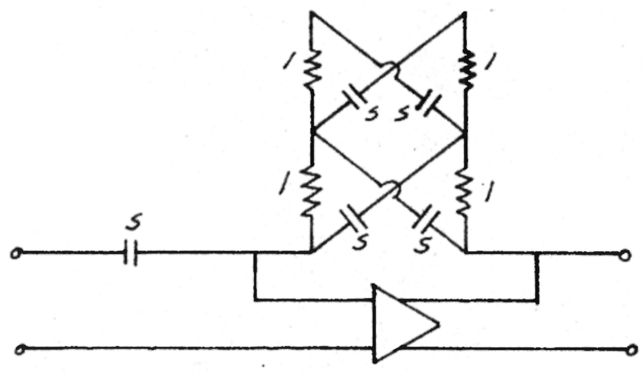

Fig. 29. Operational amplifier for approximation of $\sqrt{s}$ with lattices terminated in an open circuit for feedback networks.

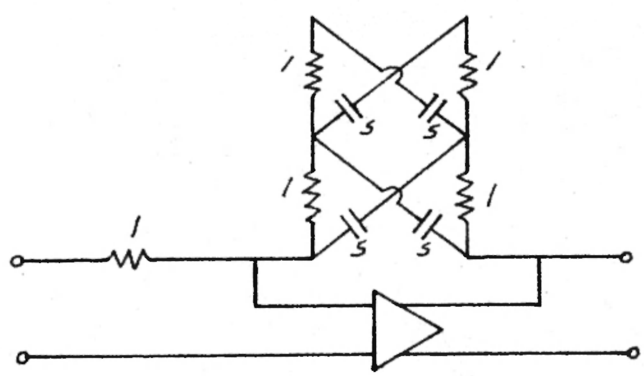

Fig. 30. Operational amplifier for approximation of $1/\sqrt{s}$ with lattices terminated in an open circuit for feedback network.

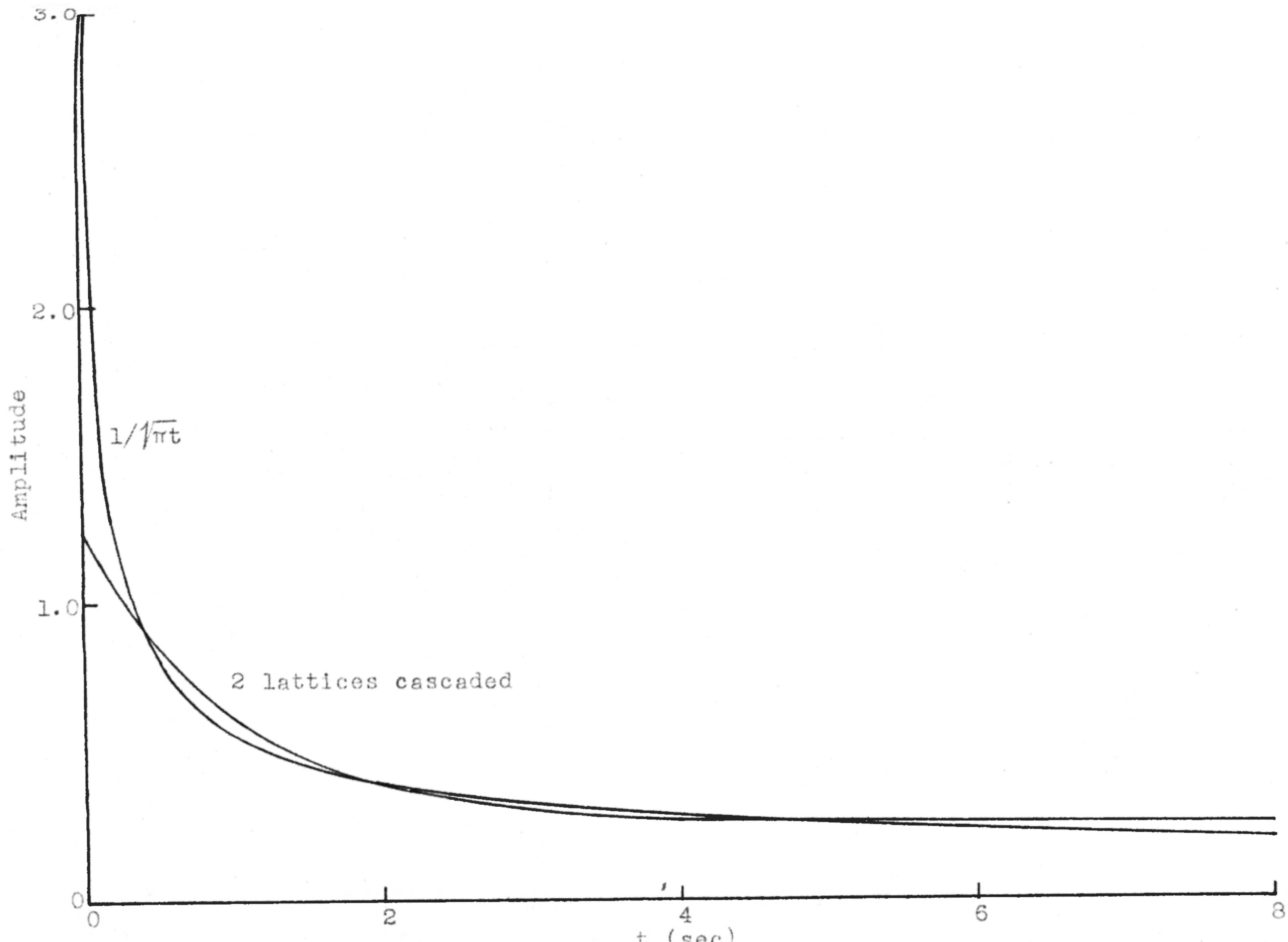

Fig. 31. Response to a unit step of approximations of $\sqrt{s}$ using open-circuited lattices.

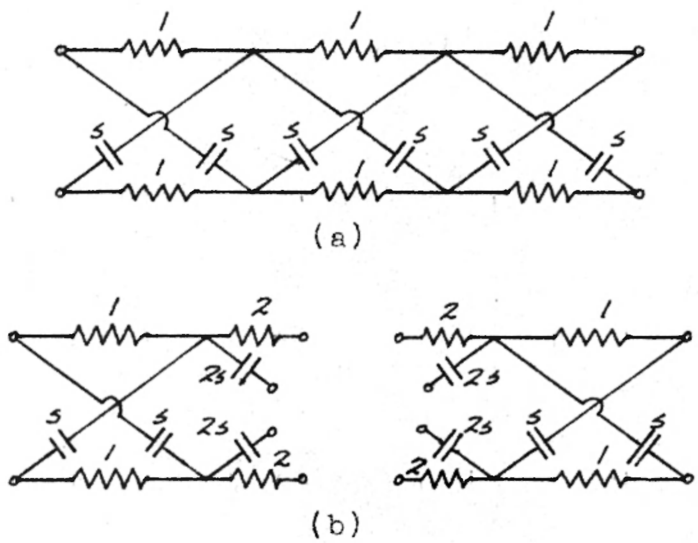

Fig. 32. (a) Three cascaded lattices;
(b) three cascaded lattices
which have been bisected.

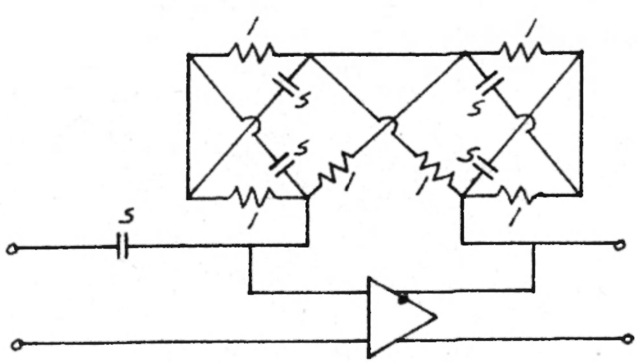

Fig. 33. Operational amplifier for first order approximation of $\sqrt[4]{s}$.

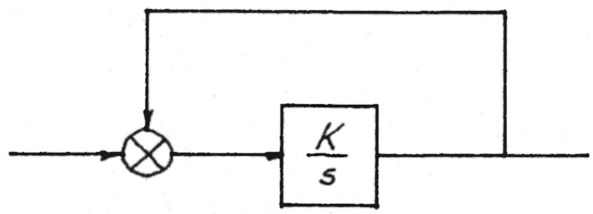

Fig. 34. Block diagram of servo of canonical form I.

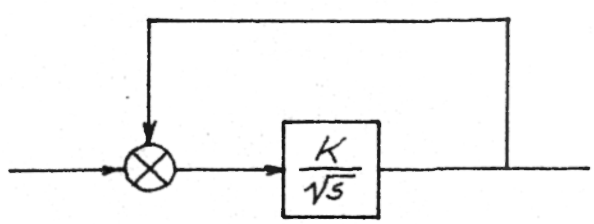

Fig. 35. Block diagram of servo of canonical form II.

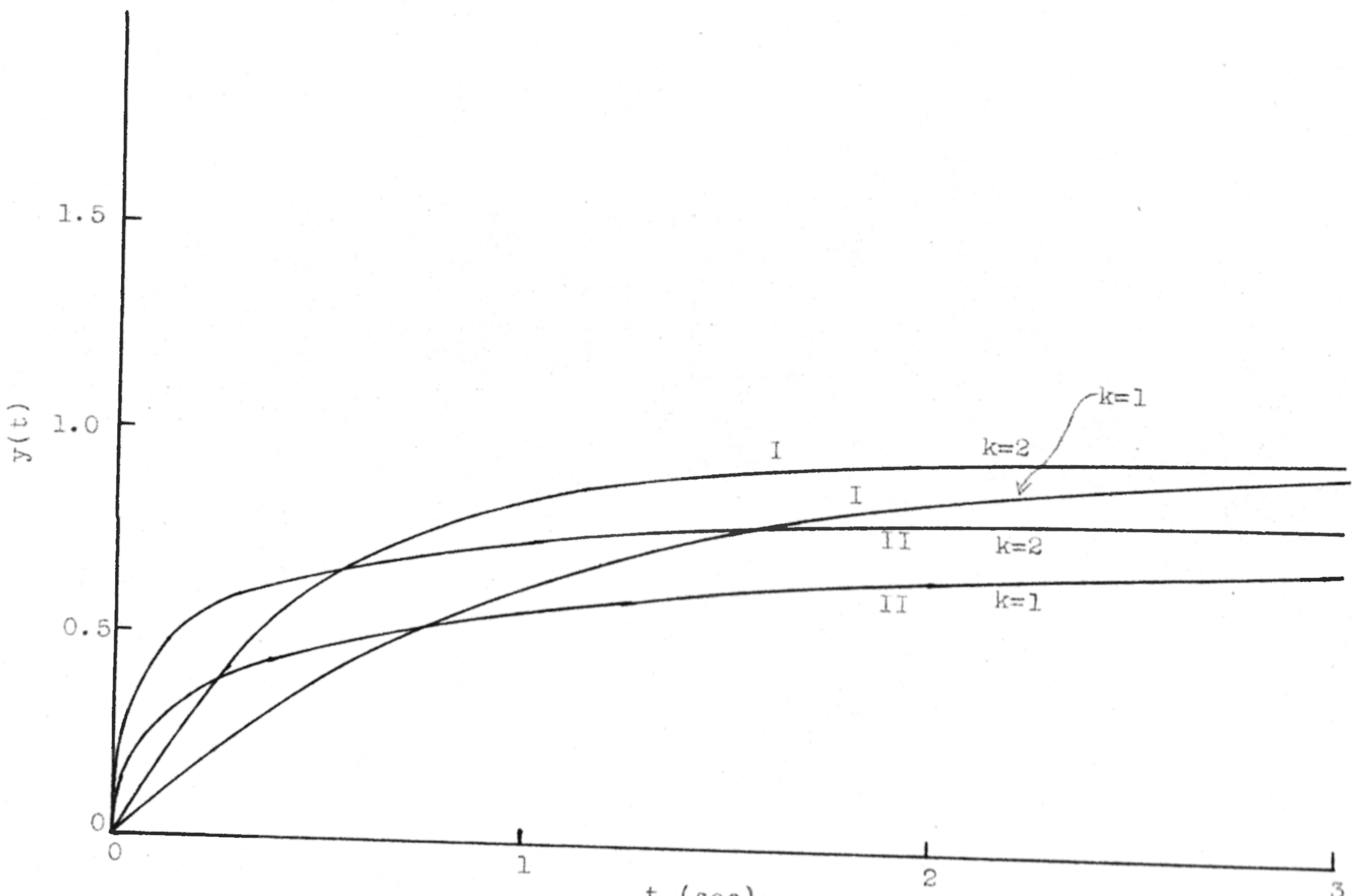

Fig. 36. Response to a unit step input of servos of canonical forms I and II.

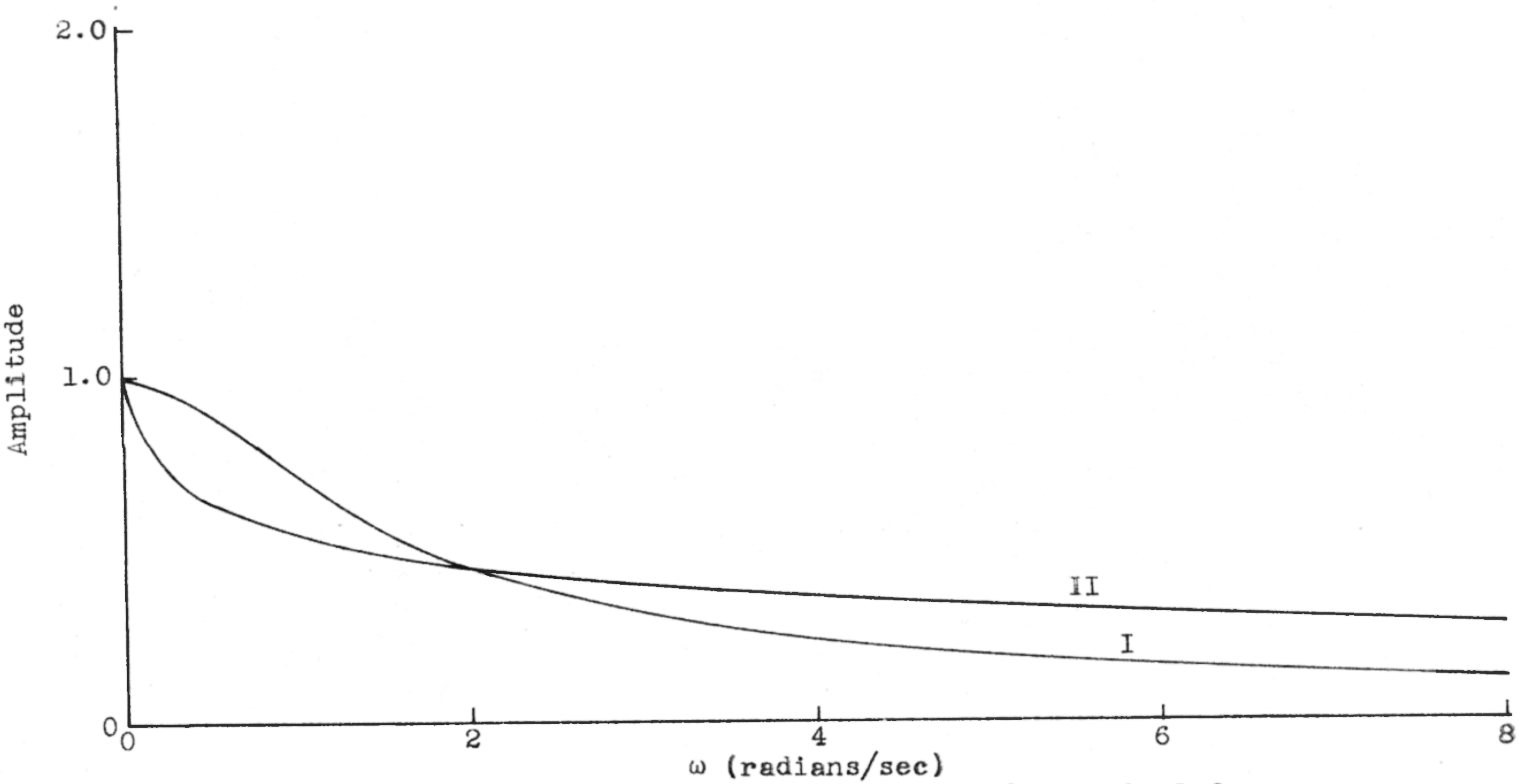

Fig. 37. Frequency response of servos of canonical forms I and II with gain equal to 1.

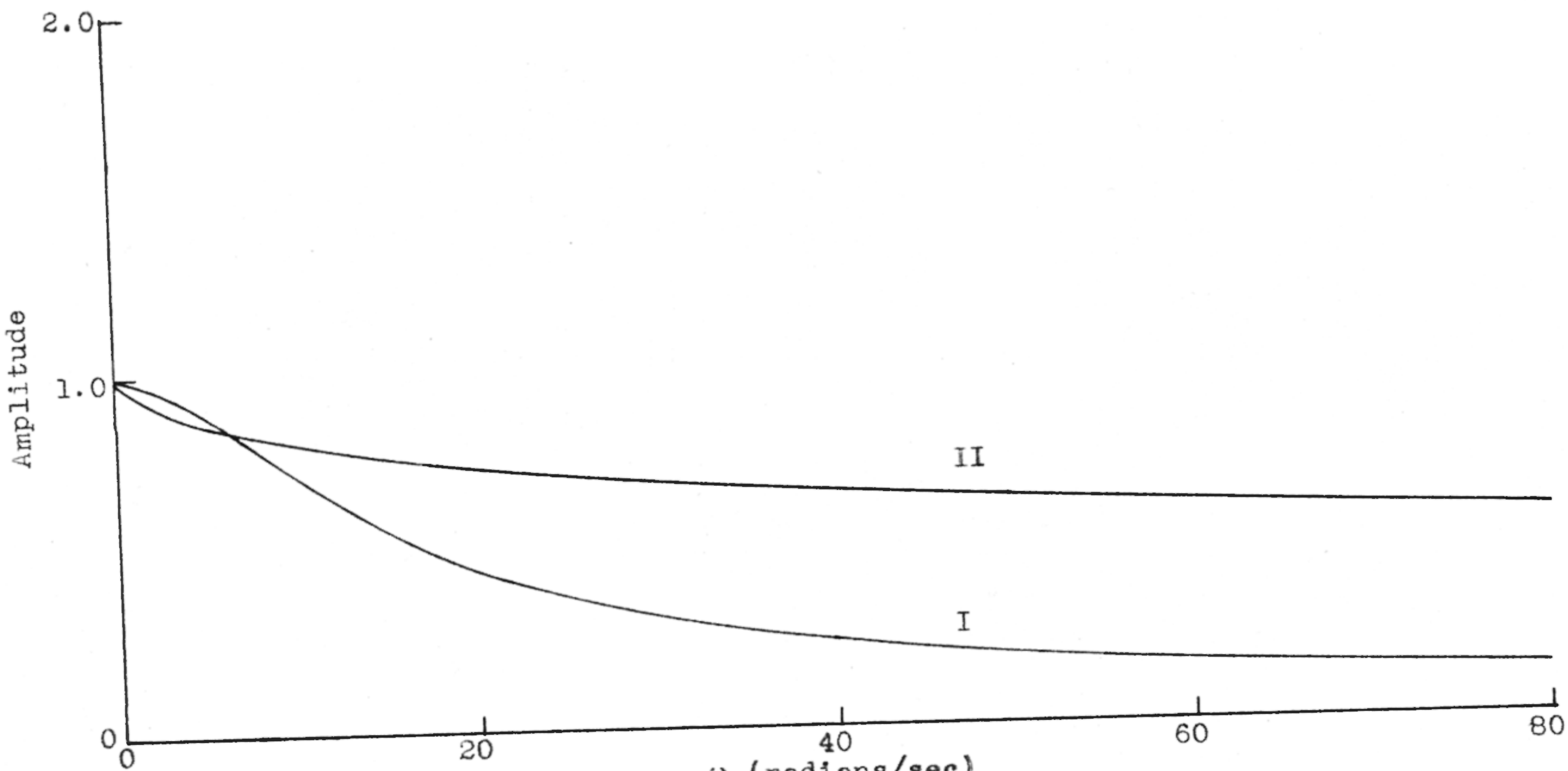

Fig. 38. Frequency response of servos of canonical forms I and II with gain of 10.

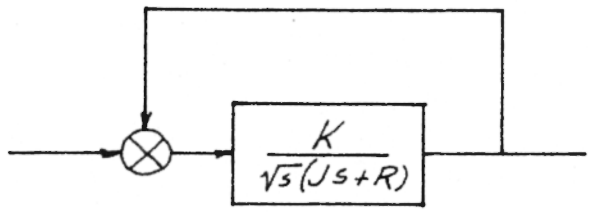

Fig. 39. Block diagram of a position servo with fractional derivative compensation.

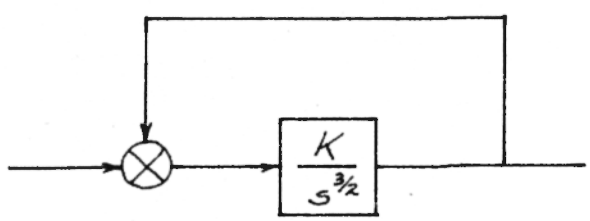

Fig. 40. Approximate form of a position servo with low damping and fractional integral compensation.

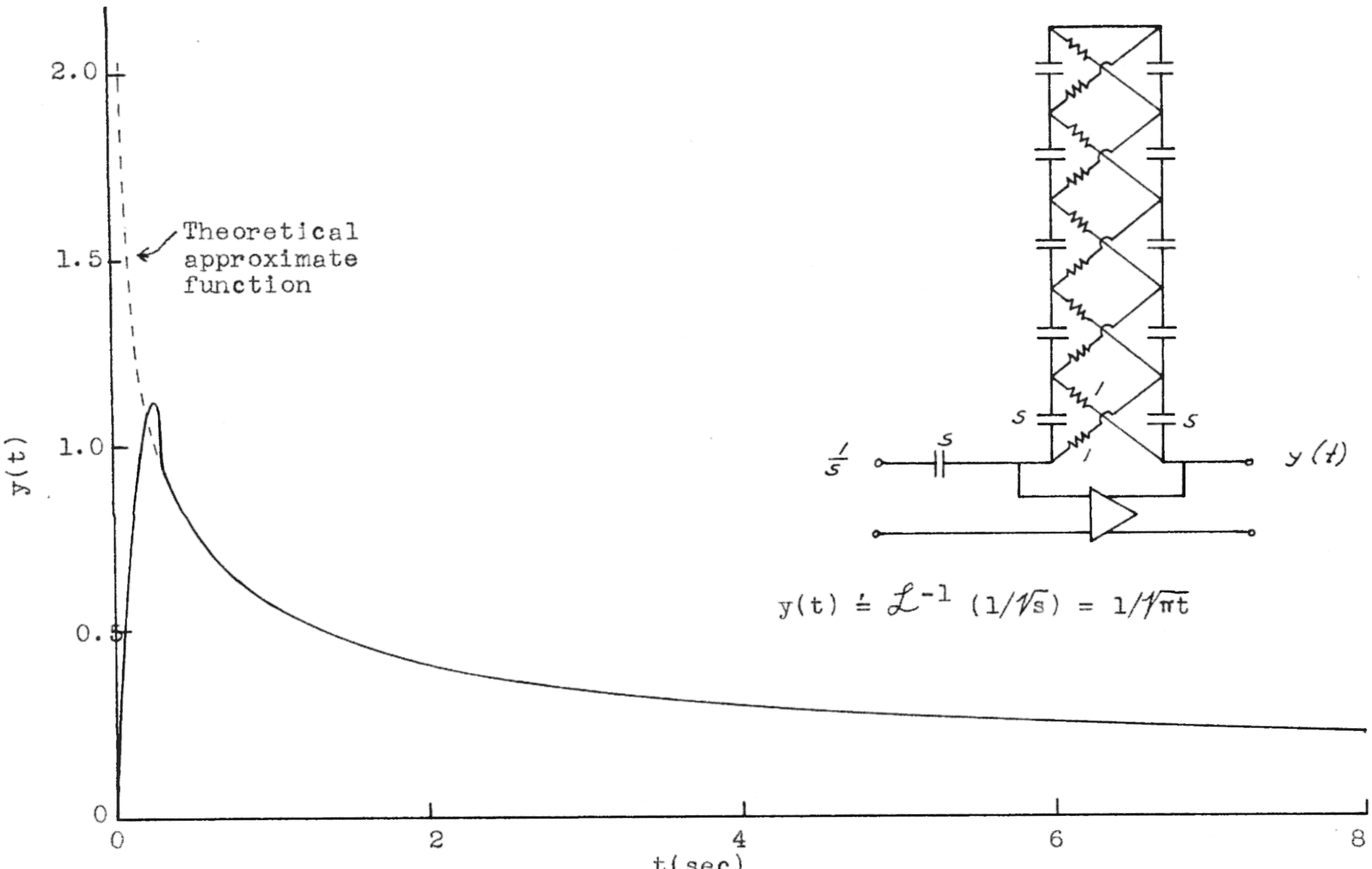

Fig. 41. Computer simulation of the response of the approximate operator $\sqrt{s}$.

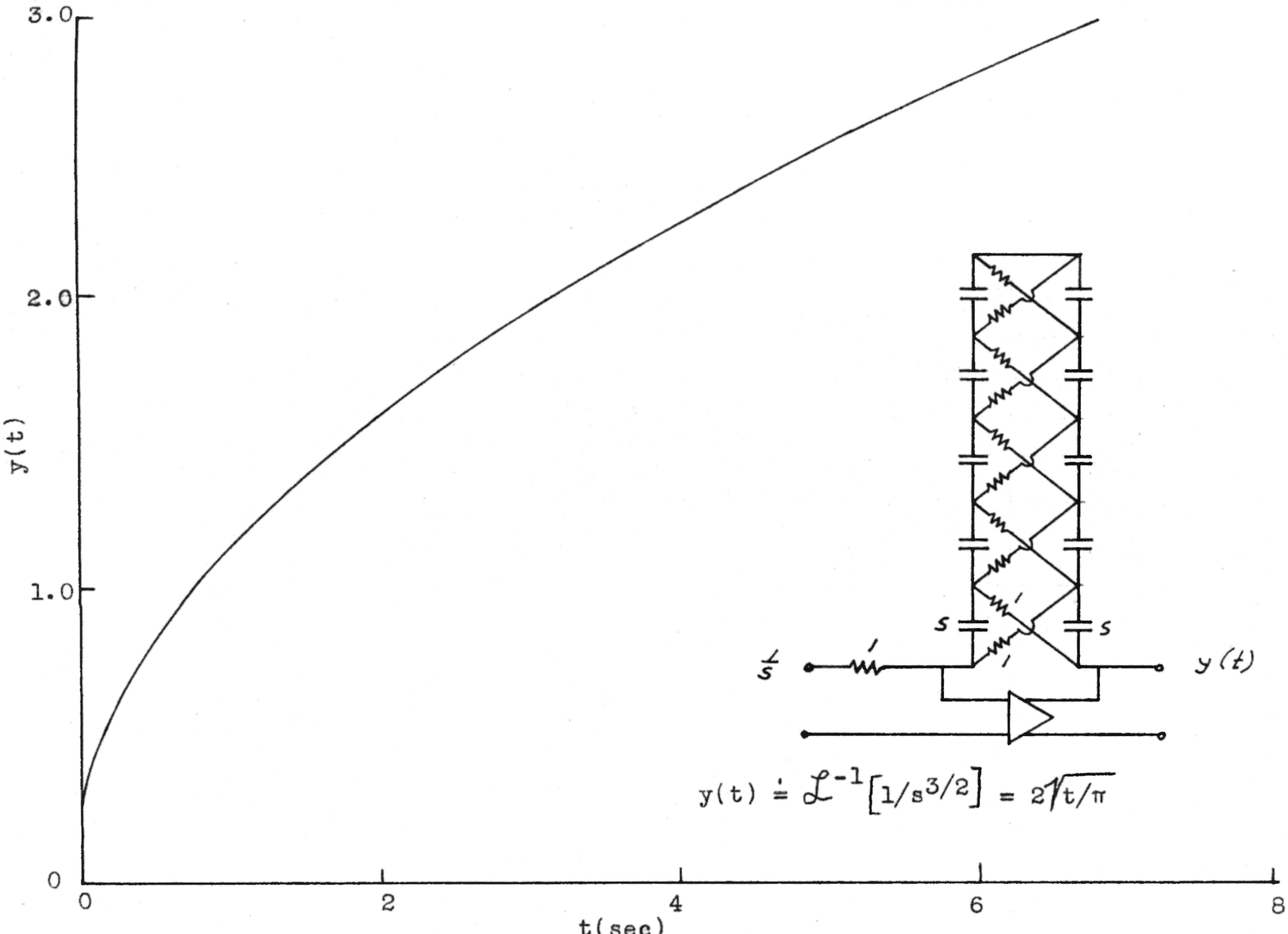

Fig. 42. Computer simulation of the response of the approximate operator $1/\sqrt{s}$.

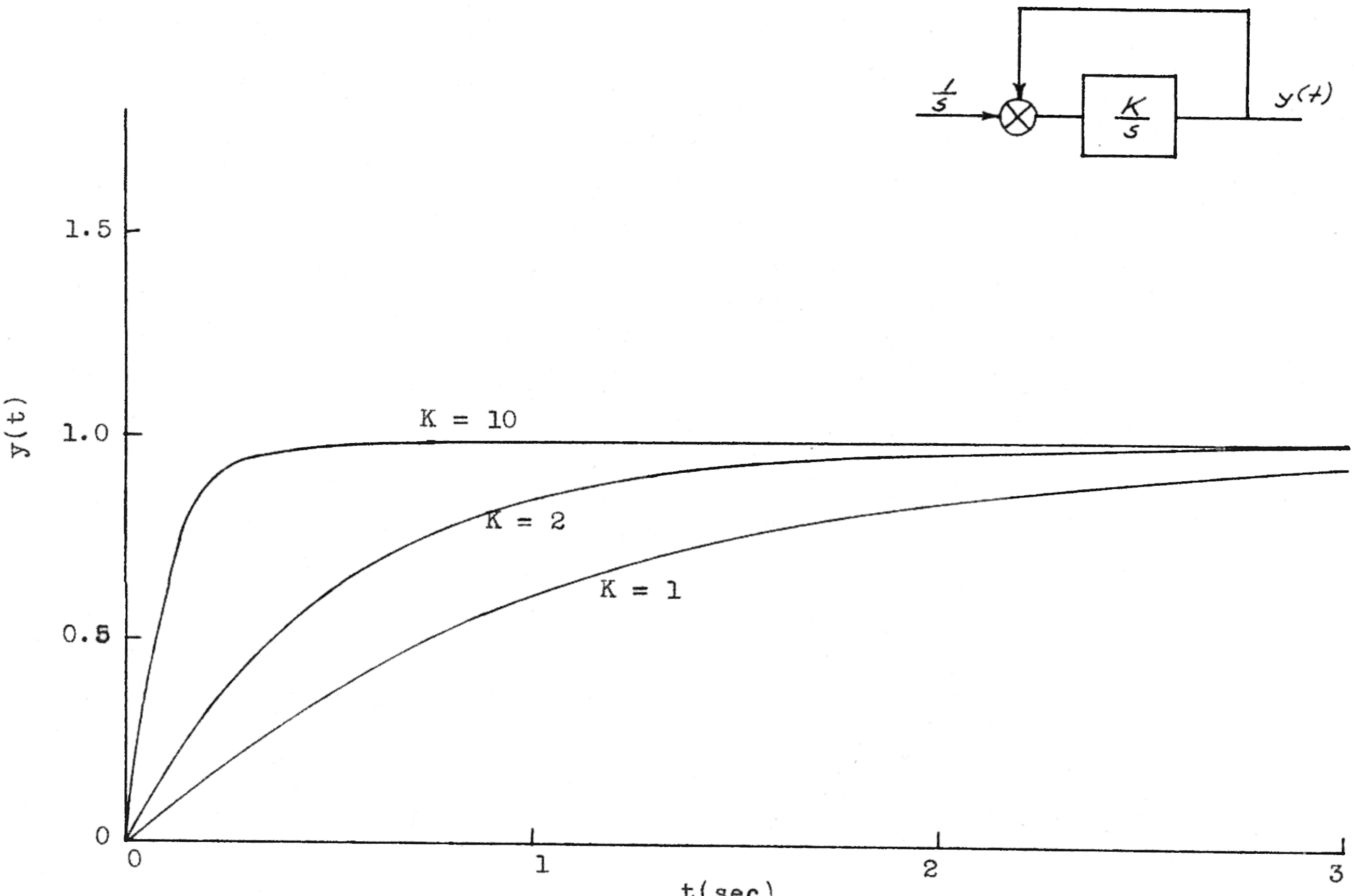

Fig. 43. Response of a servo of canonical form I to a unit step input.

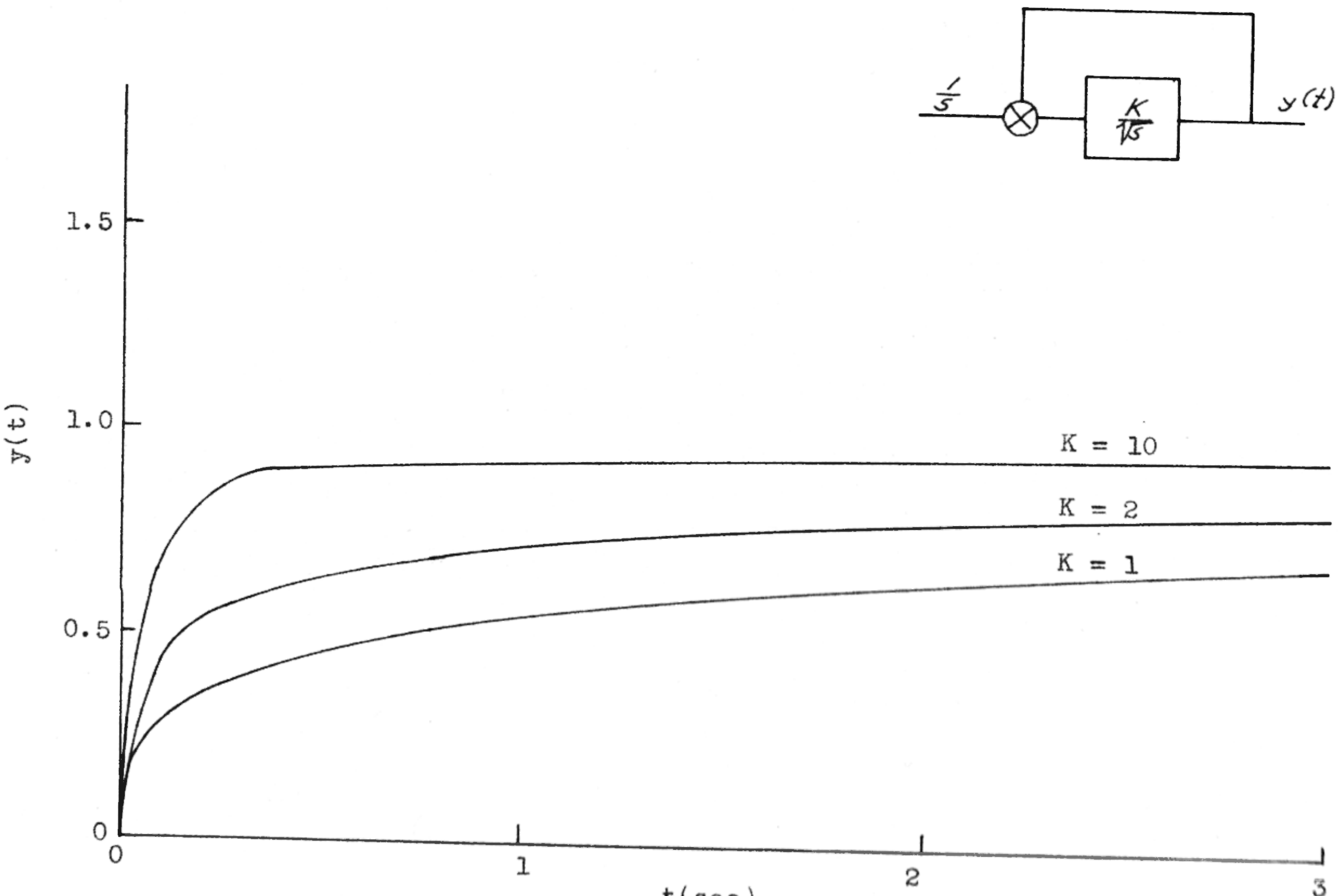

Fig. 44. Response of a servo of canonical form II to a unit step input.

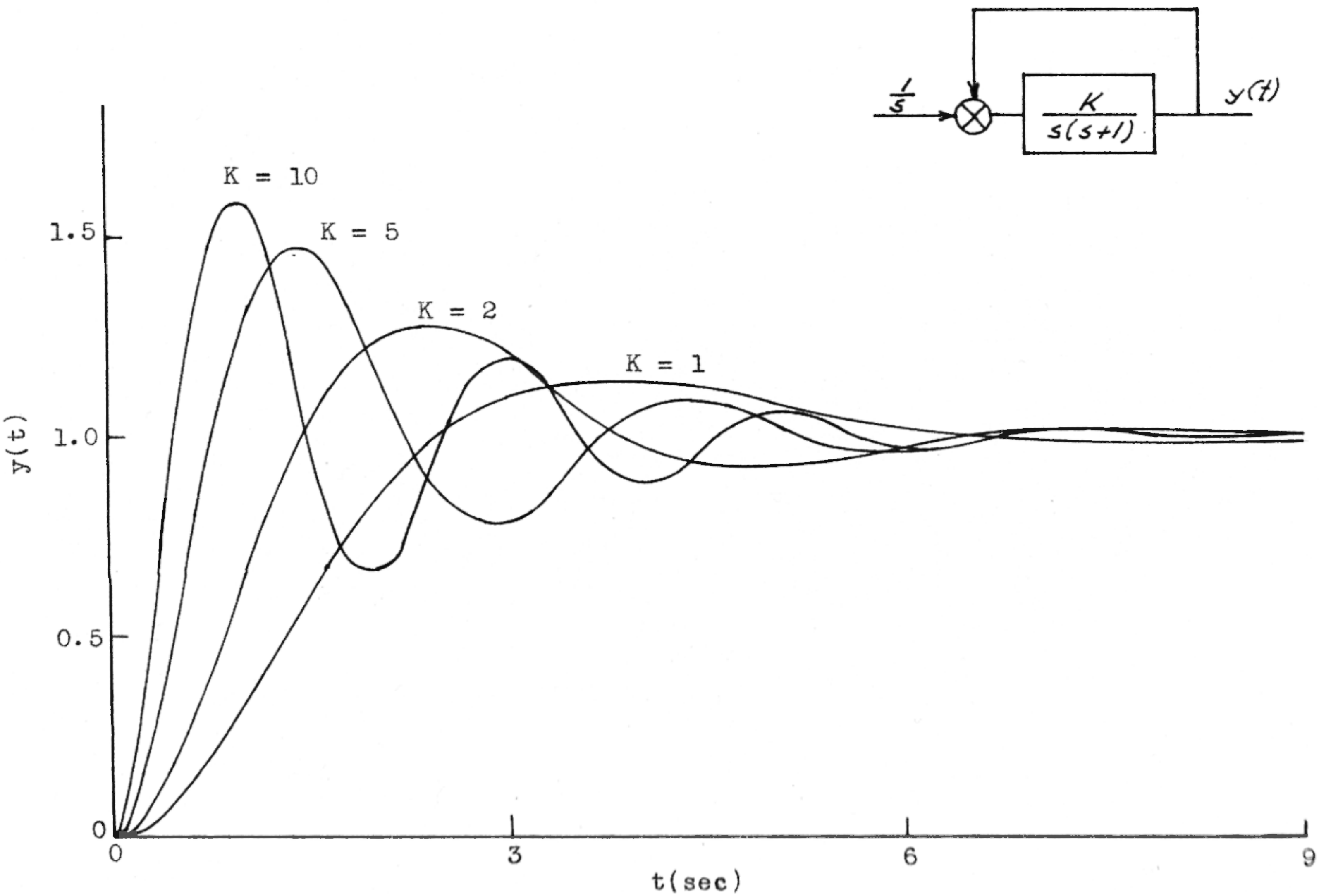

Fig. 45. Response of a position servo to a unit step input.

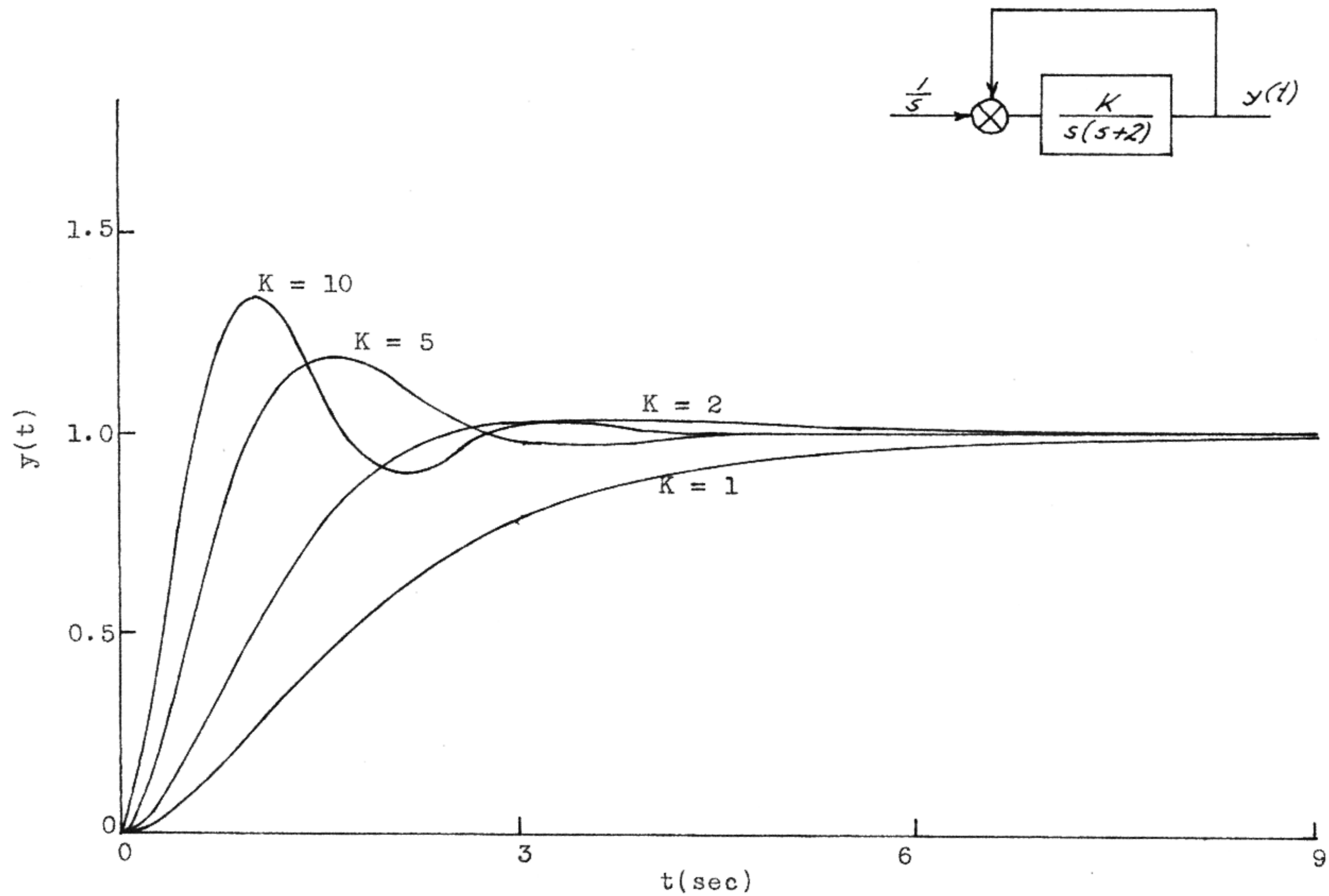

Fig. 46. Response of a position servo to a unit step input.

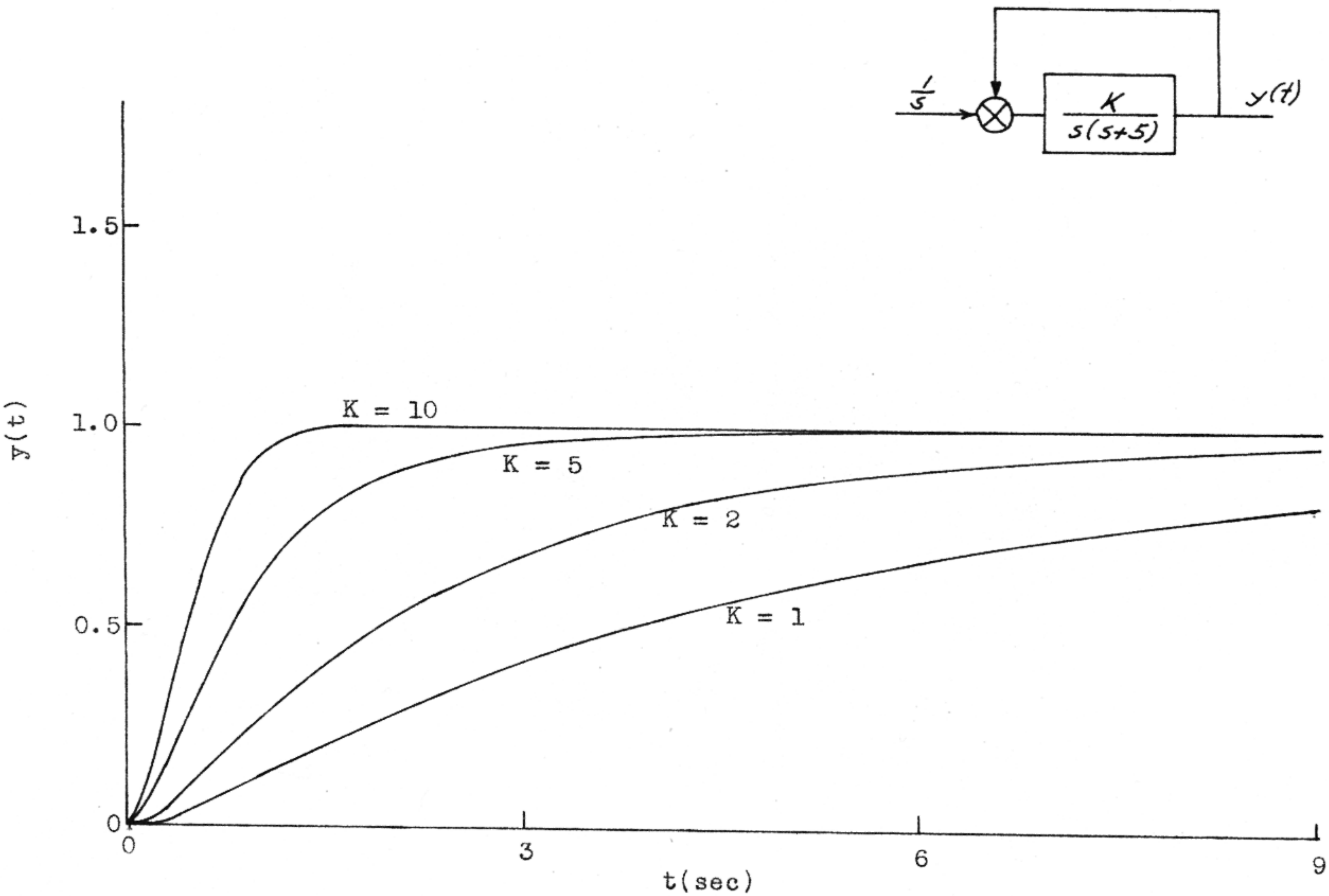

Fig. 47. Response of a position servo to a unit step input.

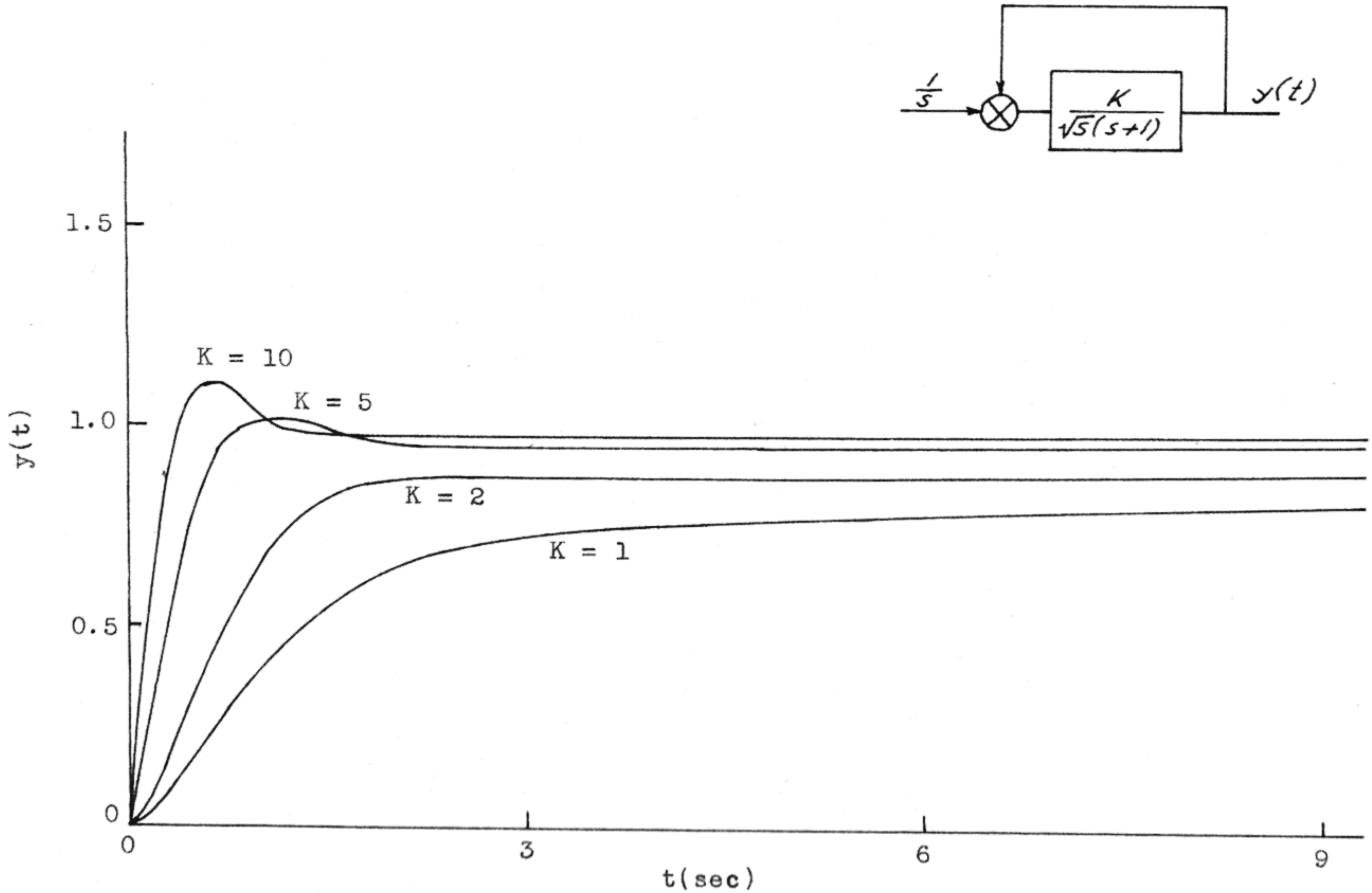

Fig. 48. Response to a unit step input of a position servo with fractional derivative compensation.

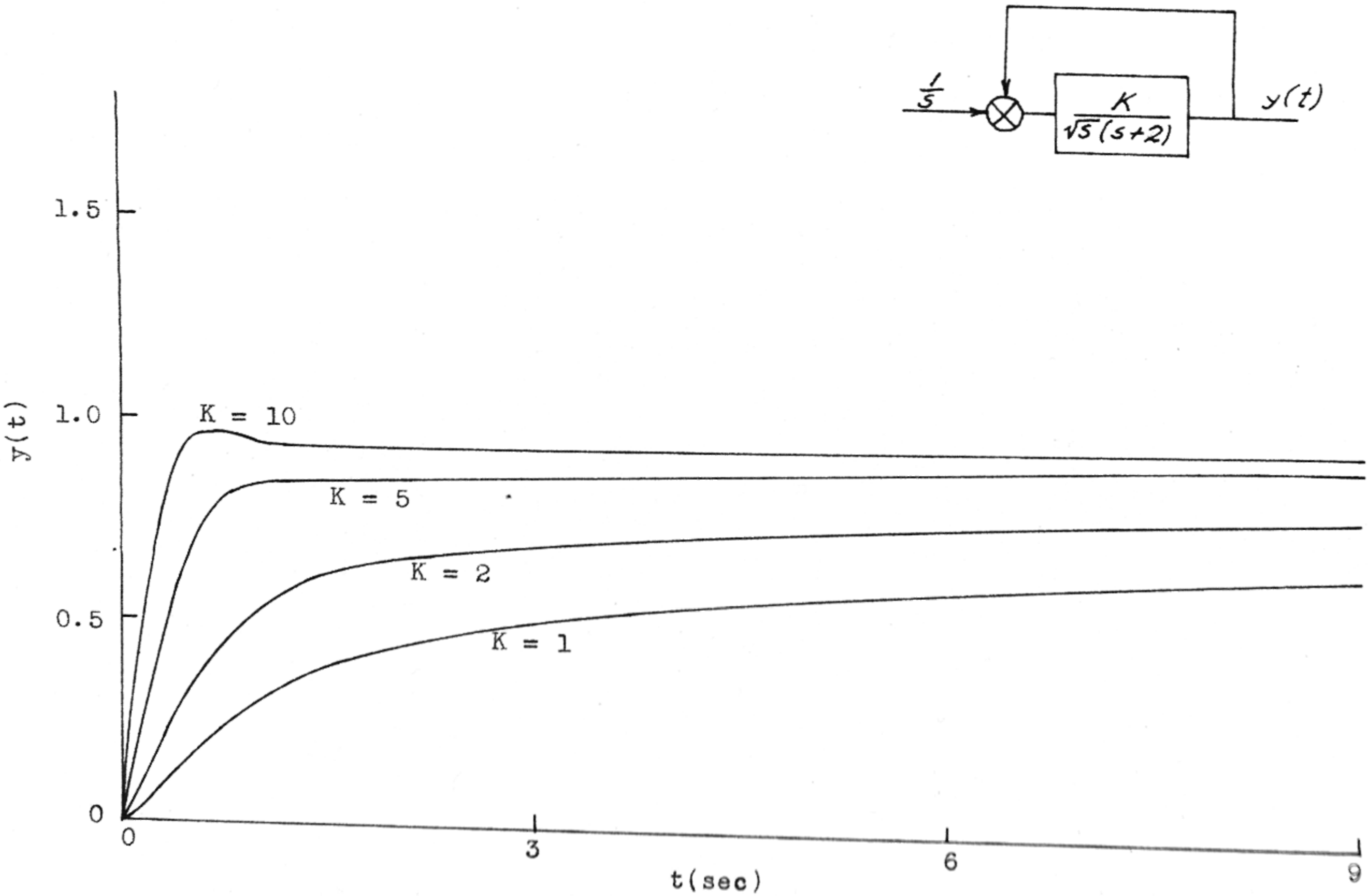

Fig. 49. Response to a unit step input of a position servo with fractional derivative compensation.

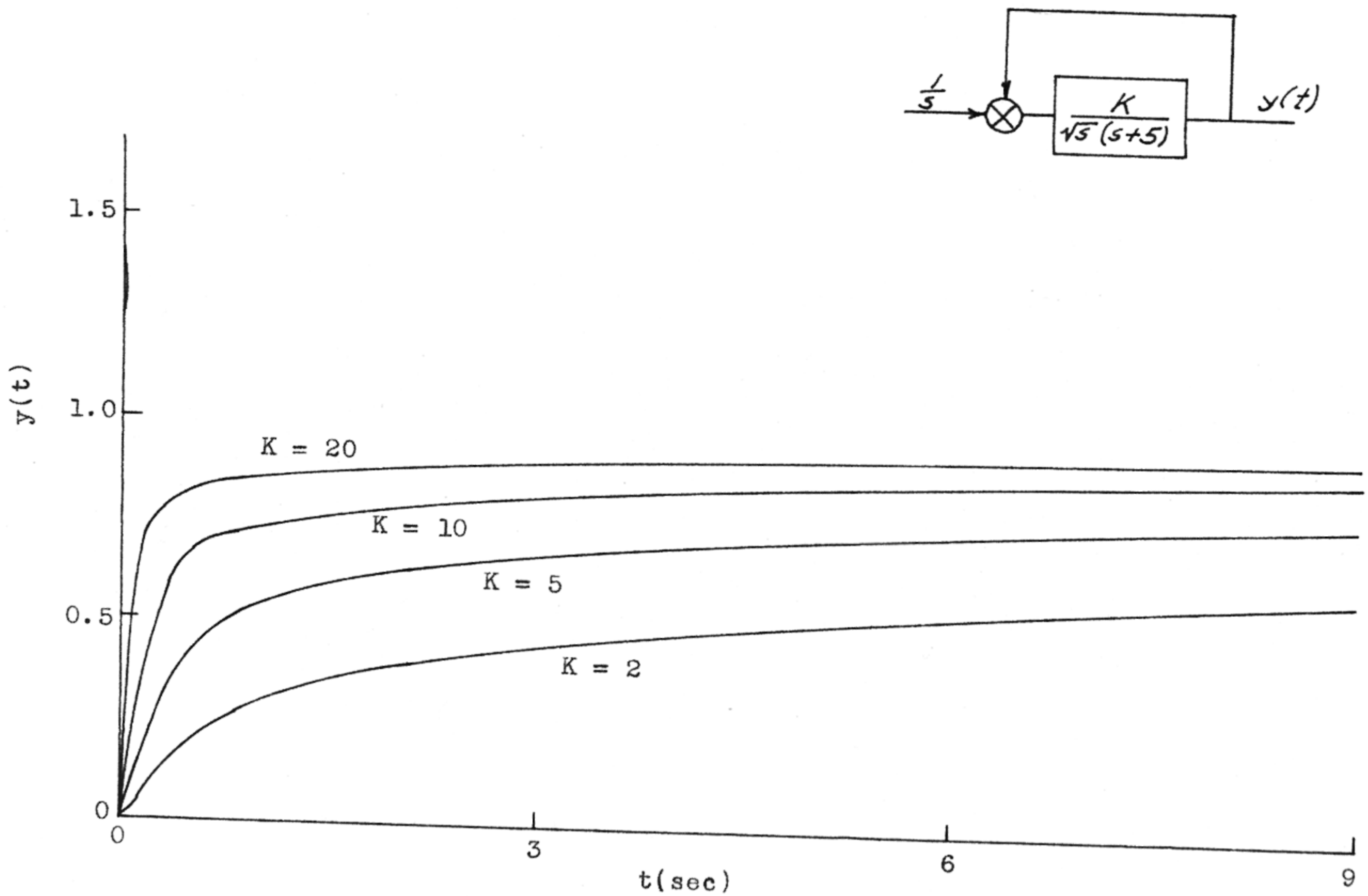

1/s
K / √s (s+5)
y(t)
1.5
1.0
0.5
0
y(t)
K = 20
K = 10
K = 5
K = 2
0
3
6
9
t(sec)

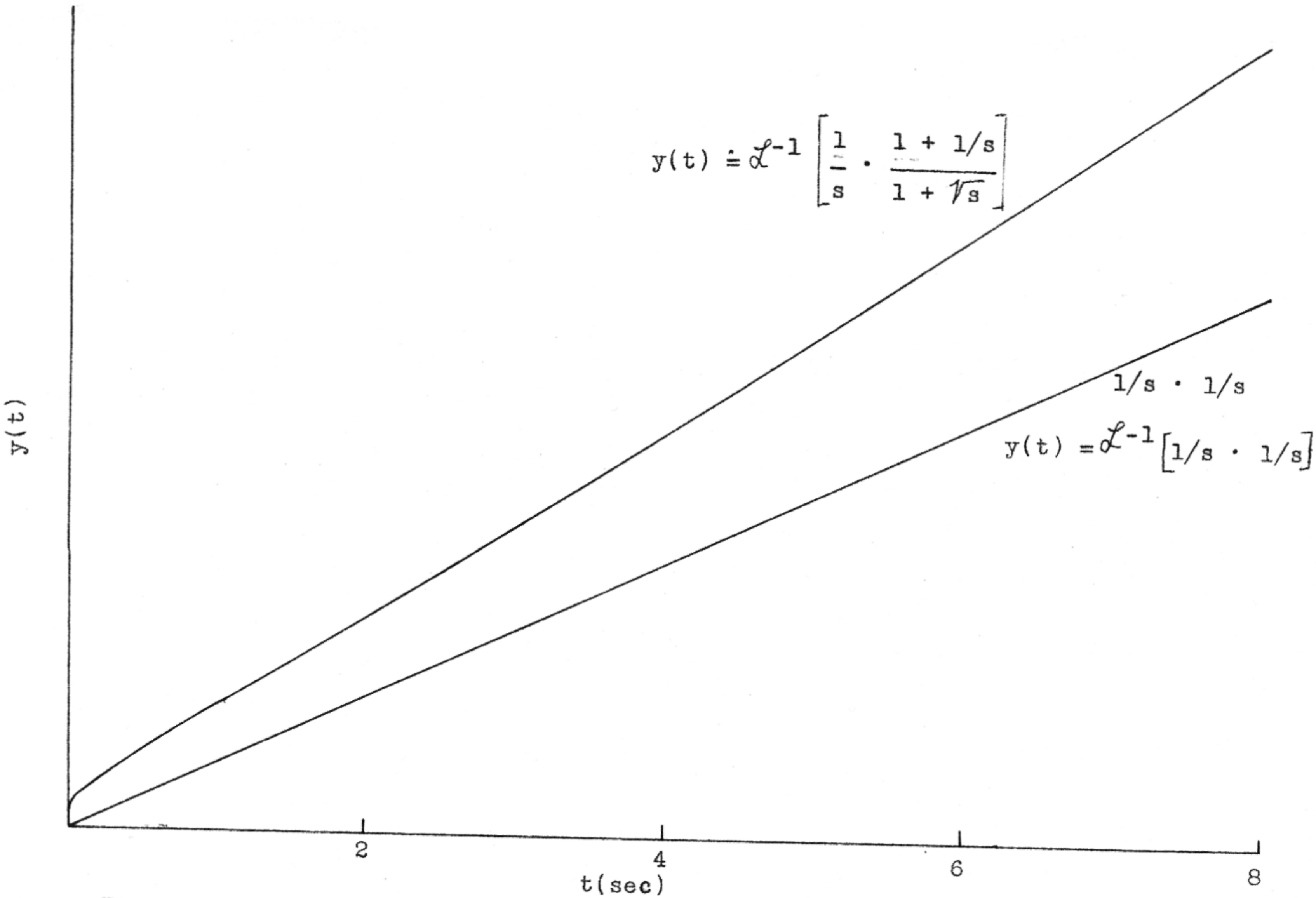

Fig. 51. Response of the self-averaging function to a unit step input compared with the response of an integrator to a unit step input.

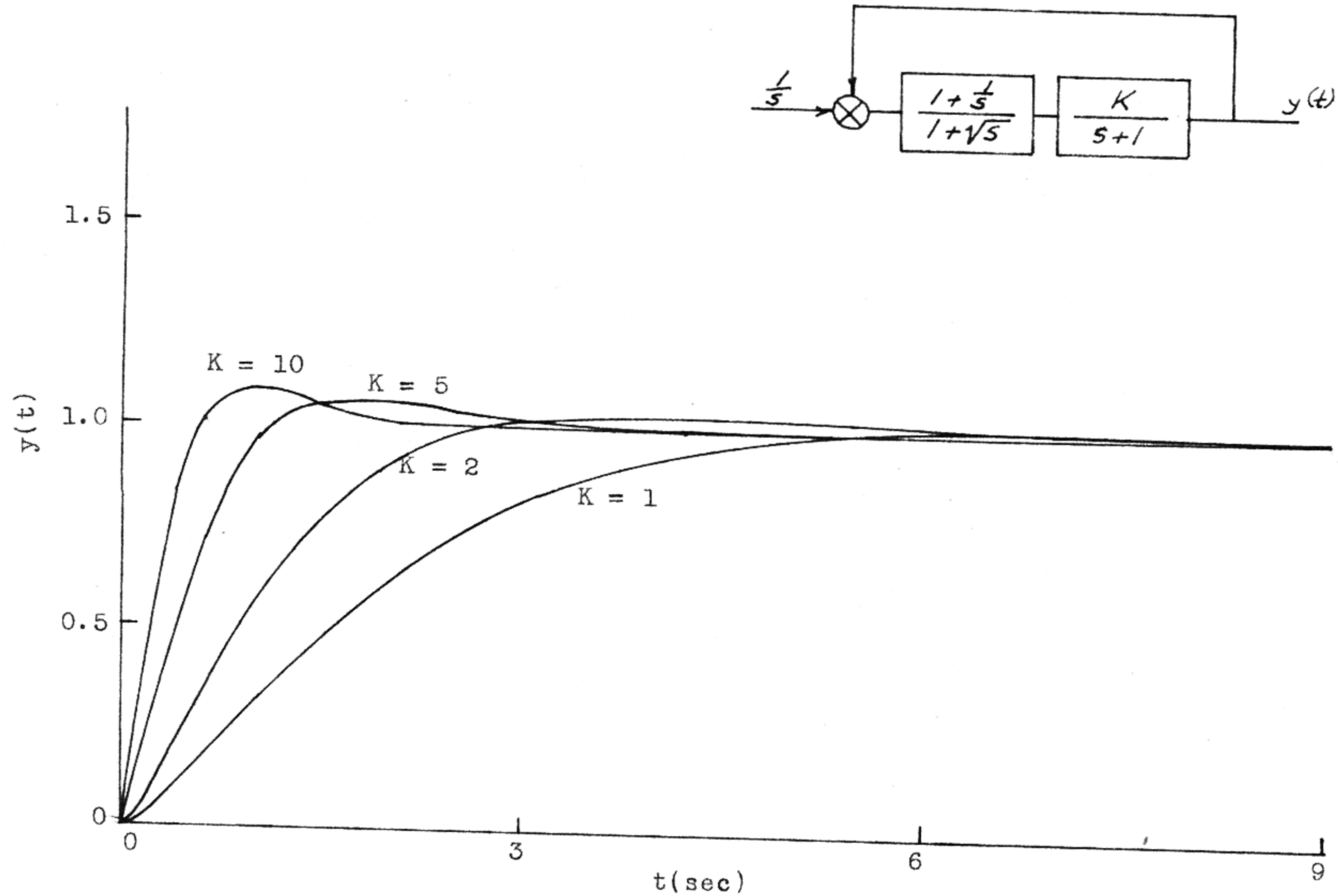

Fig. 52. Response to a unit step input of a position servo with self-averaging fractional derivative compensation.

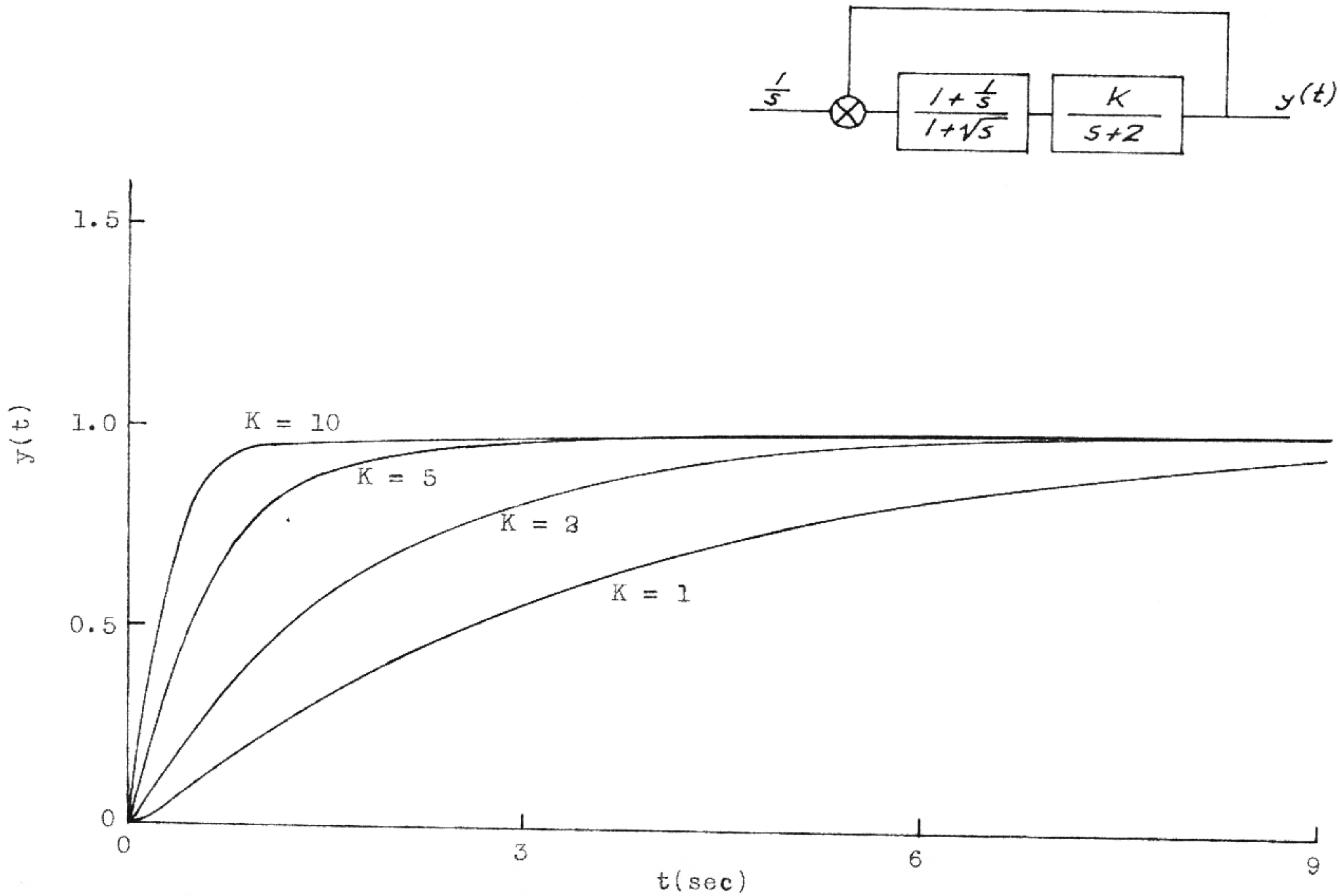

Fig. 53. Response to a unit step input of a position servo with self-averaging fractional derivative compensation.

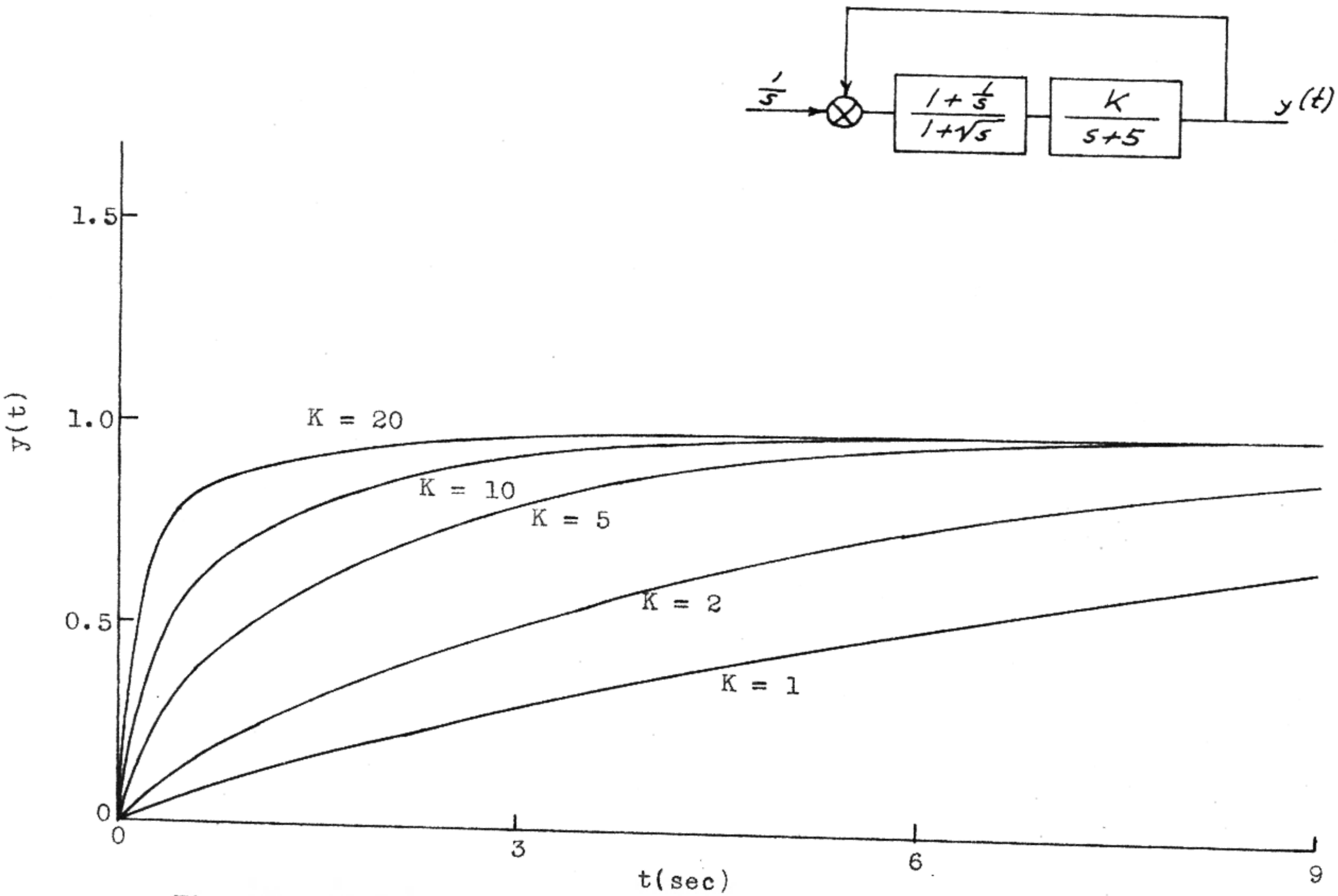

Fig. 54. Response to a unit step input of a position servo with self-averaging fractional derivative compensation.

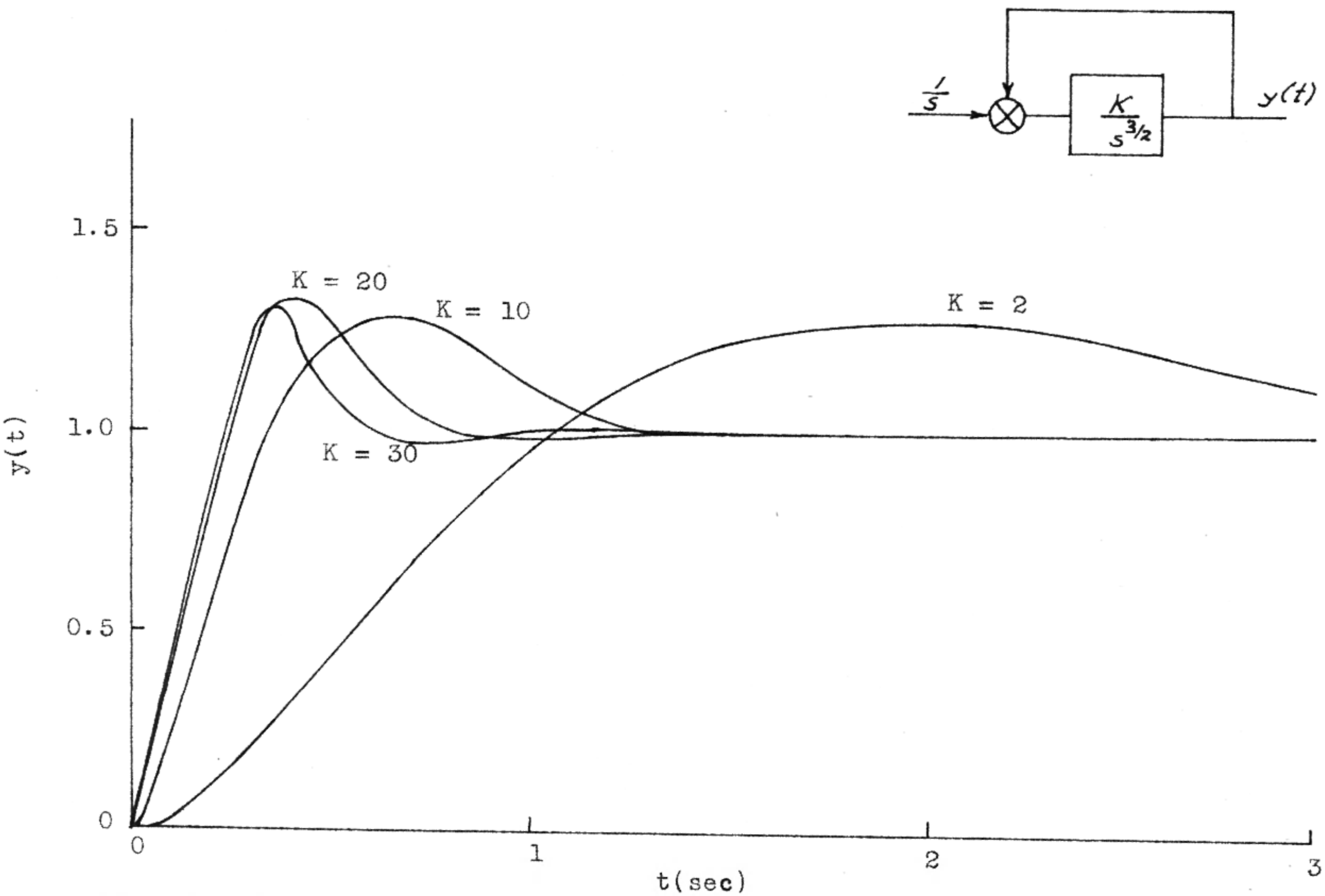

Fig. 55. Response to a unit step input of the approximate form of a position servo with low damping and fractional integral compensation.

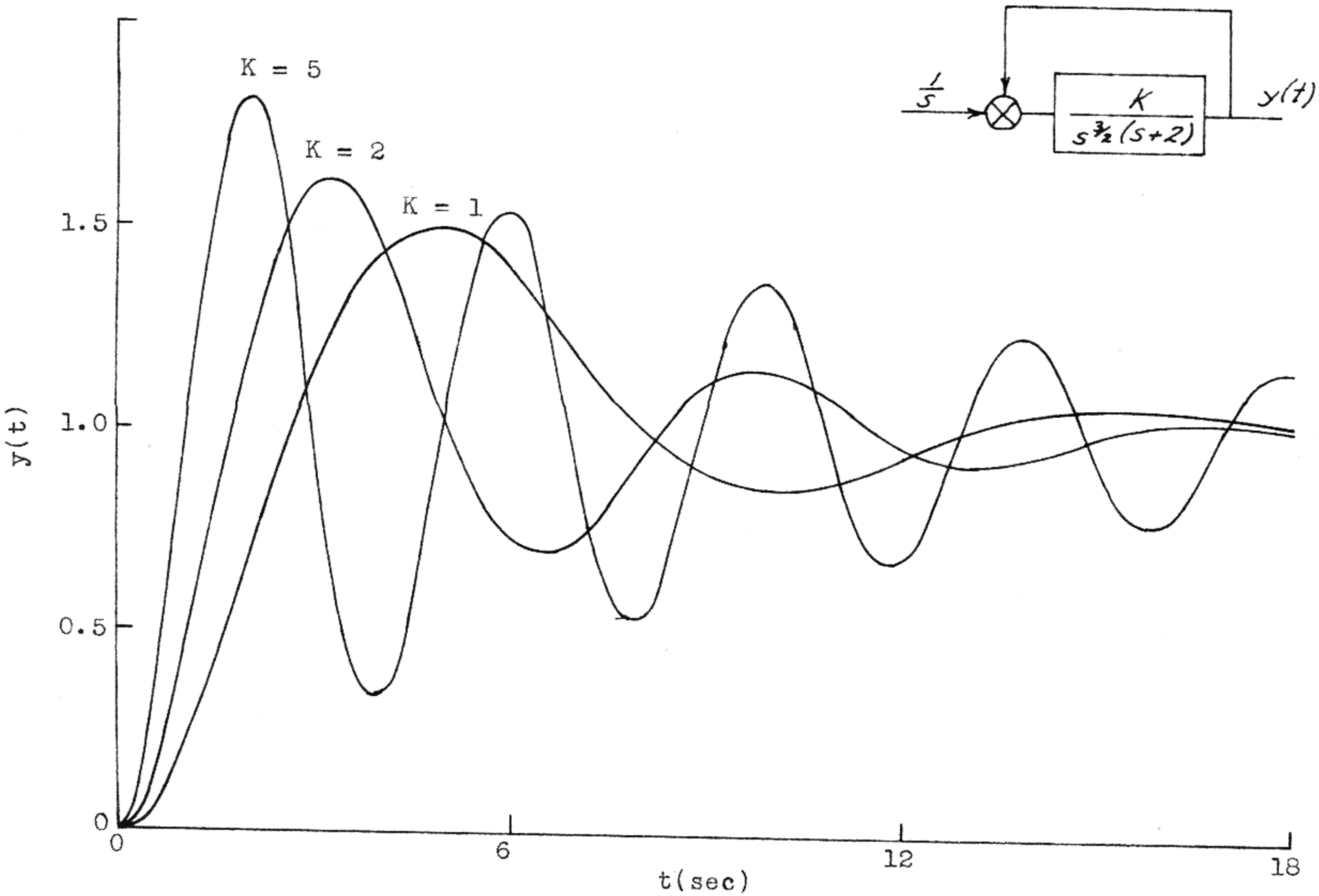

Fig. 56. Response to a unit step input of a position servo with fractional integral compensation.

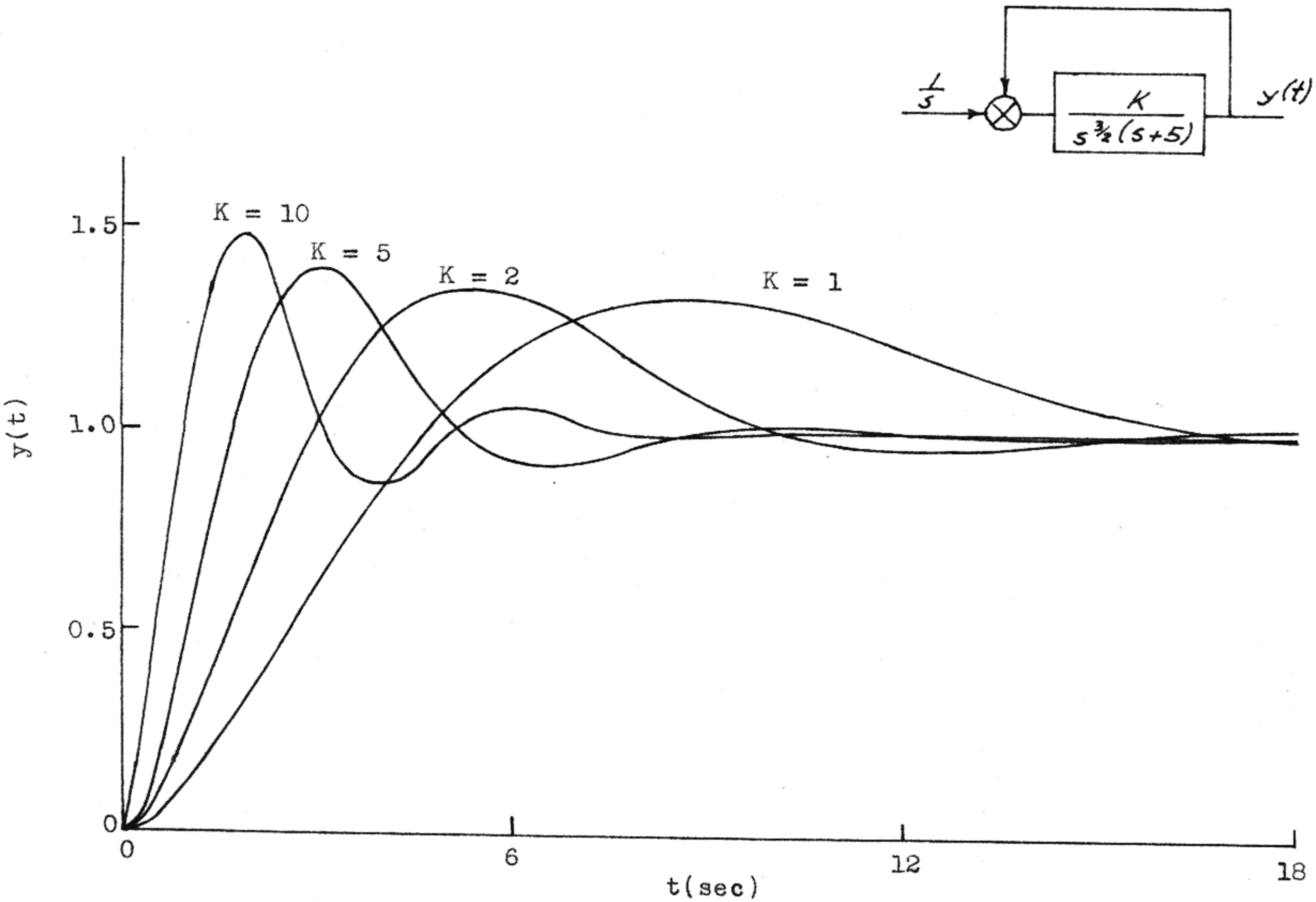

Fig. 57. Response to a unit step input of a position servo with fractional integral compensation.

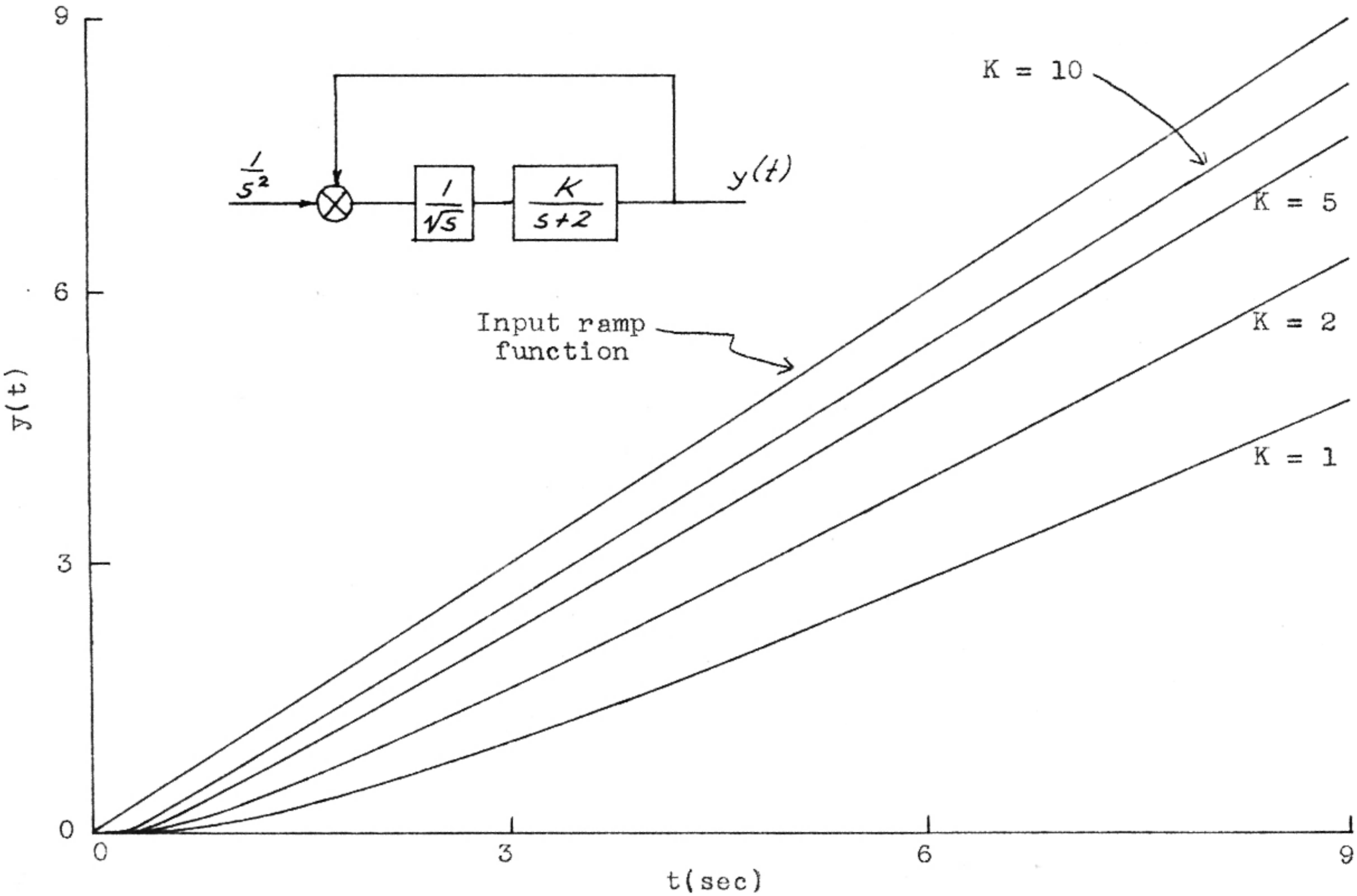

Fig. 58. Response to a ramp function input of a velocity servo with fractional integral compensation.

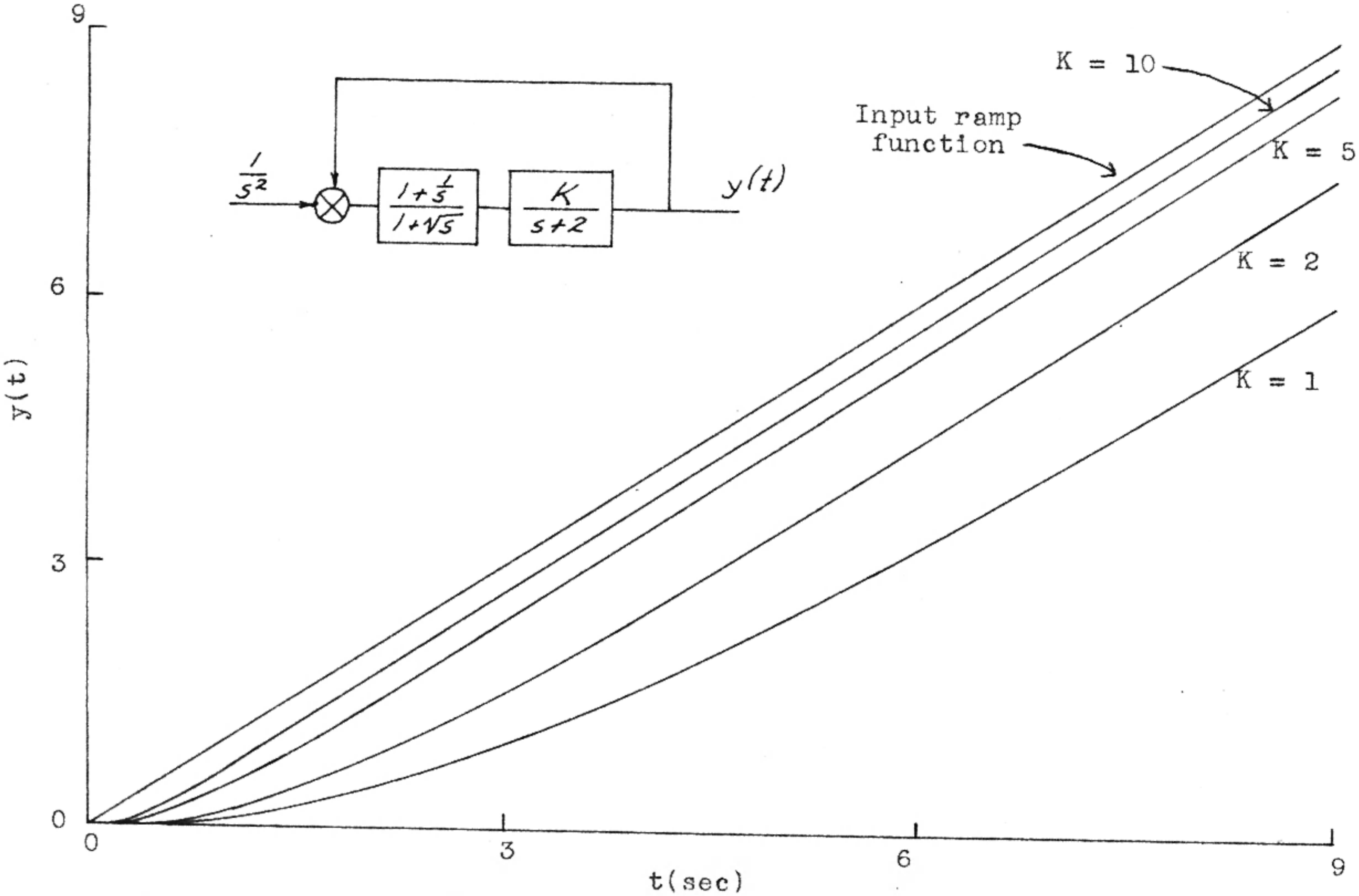

Fig. 59. Response to a ramp function input of a velocity servo with self-averaging fractional integral and integral compensation.

SIMULATION OF THE FRACTIONAL DERIVATIVE
OPERATOR $\sqrt{s}$ AND THE FRACTIONAL
INTEGRAL OPERATOR $1/\sqrt{s}$

by

GORDON EUGENE CARLSON

B. S., Kansas State University
of Agriculture and Applied Science, 1959

AN ABSTRACT OF
A MASTER'S REPORT

submitted in partial fulfillment of the

requirements for the degree

MASTER OF SCIENCE

Department of Electrical Engineering

KANSAS STATE UNIVERSITY
OF AGRICULTURE AND APPLIED SCIENCE

1960

The purpose of this paper is to approximate the operators $\sqrt{s}$ and $1/\sqrt{s}$. A necessary preliminary to the approximating procedure is a study of the linear adaptive servo. The linear adaptive servo is analyzed with both derivative feedback control and integral feedback control. If the transfer function for this servo has large feedback gain, then the Newton and Lanczos approximations to the fractional derivative and fractional integral operators may be simulated.

These approximations may be readily realized on operational amplifiers. The networks developed for the feedback loop of these operational amplifiers consist of cascaded lattice networks with resistors and capacitors. The characteristic admittance of these lattices is $\sqrt{s}$; therefore in the limiting case of infinite number of lattices in cascade, the functions $\sqrt{s}$ and $1/\sqrt{s}$ would be simulated. Both approximation functions are simulated by truncating the number of lattices in cascade.

The fractional operators can be used in several different applications. They can be used in the analog simulation of heat transfer problems and neutron diffusion problems. Application of these operators to servo compensation is demonstrated. The fractional derivative compensation of a position servo gives a higher initial slope than the uncompensated servo has, eliminates most of the oscillation in servos with a low damping factor, and has zero steady-state error. Fractional derivative compensation has the disadvantage of giving a slower approach to the steady-state condition after its initial high slope than does the uncompensated servo. A better result is obtained by using a self average of the fractional derivative and the identity transfer functions. This average incorporates the good points of each.

The fractional integral compensation of a velocity servo gives no help in the elimination of velocity lag. In fact, with fractional integral compensation, the velocity lag is slow to even attain a steady-state value. The self average of integral compensation and fractional integral compensation also gives a steady-state velocity lag, though it attains steady-state conditions quicker than the servo with fractional integral compensation.

Actual analog computer simulations of the transfer functions $\sqrt{s}$ and $1/\sqrt{s}$, and the servo compensation techniques are included in the paper to substantiate the above observations.